TDDFT for excitation energies
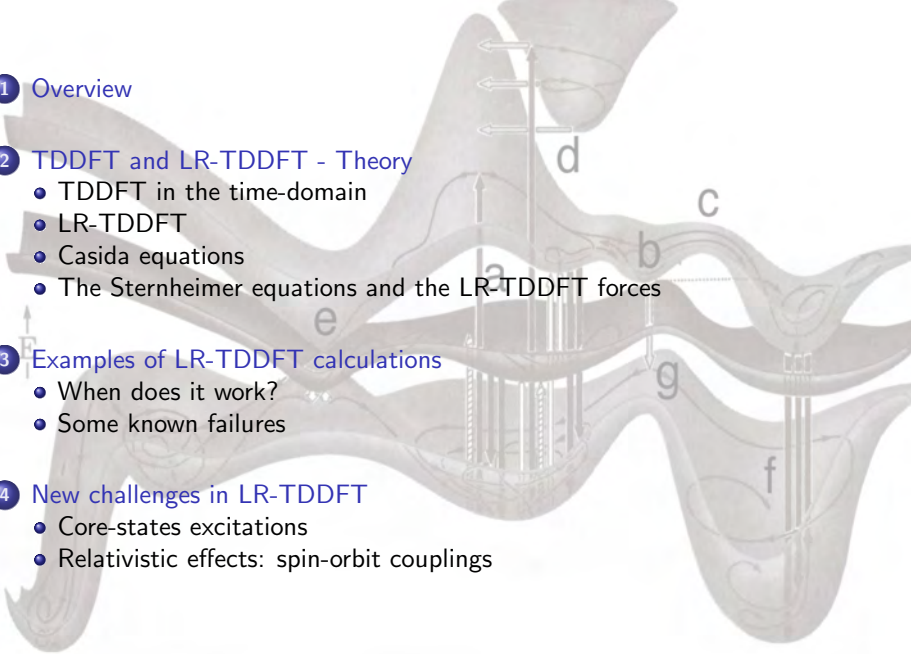## TDDFT for ultrafast electronic dynamics

Ivano Tavernelli and Basile Curchod

Laboratory of Computational Chemistry and Biochemistry, EPFL, Lausanne

TDDFT SCHOOL
BENASQUE 2014

ÉCOLE POLYTECHNIQUE
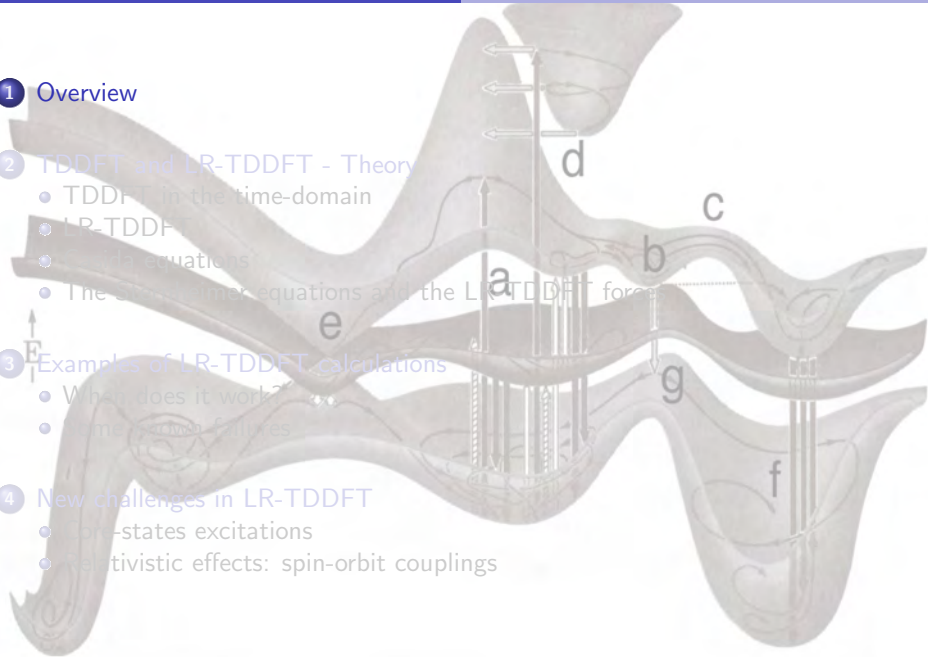FÉDÉRALE DE LAUSANNE

1 Overview

2 TDDFT and LR-TDDFT - Theory
- TDDFT in the time-domain
- LR-TDDFT
- Casida equations
- The Sternheimer equations and the LR-TDDFT forces

3 Examples of LR-TDDFT calculations
- When does it work?
- Some known failures

# 4 New challenges in LR-TDDFT
- Core-states excitations
- Relativistic effects: spin-orbit couplings

Chemistry is about atomic rearrangements

From Wikipedia:

Chemistry (from Egyptian keme (chem), meaning "earth") is the science concerned with the composition, structure, and properties of matter, as well as the changes it undergoes during chemical reactions. Historically, modern chemistry evolved out of alchemy following the chemical revolution (1773). Chemistry is a physical science related to studies of various atoms, molecules, crystals and other aggregates of matter whether in isolation or combination, which incorporates the concepts of energy and entropy in relation to the spontaneity of chemical processes.

$[NH_4^+][NCO^-]$
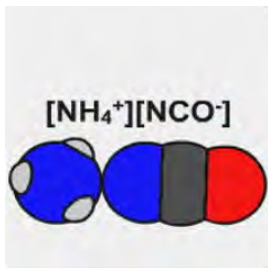
Chemistry is about atomic rearrangements

We need dynamics to model chemical reactions ....

(Sterol synthesis)

Chemistry is about atomic rearrangements

... and a way to describe the interaction with the environment.

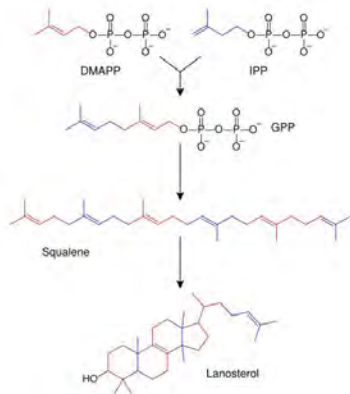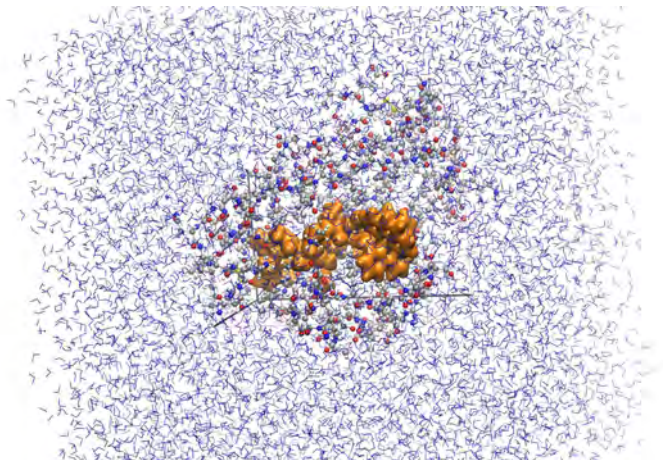# Chemistry is about atomic rearrangements

From Wikipedia:

Chemistry (from Egyptian keme (chem), meaning "earth") is the science concerned with the composition, structure, and properties of matter, as well as the changes it undergoes during chemical reactions. Historically, modern chemistry evolved out of alchemy following the chemical revolution (1773). Chemistry is a physical science related to studies of various atoms, molecules, crystals and other aggregates of matter whether in isolation or combination, which incorporates the concepts of energy and entropy in relation to the spontaneity of chemical processes.

A theoretical/computational approach will therefore need:

- theoretical model for matter in the energy range [0 to few hundred of eV]
- description of chemical reactions (structural changes)
- description of the interaction with the environment (condensed phase)

Chemistry is about atomic rearrangements

From Wikipedia:

Chemistry (from Egyptian keme (chem), meaning "earth") is the science concerned with the composition, structure, and properties of matter, as well as the changes it undergoes during chemical reactions. Historically, modern chemistry evolved out of alchemy following the chemical revolution (1773). Chemistry is a physical science related to studies of various atoms, molecules, crystals and other aggregates of matter whether in isolation or combination, which incorporates the concepts of energy and entropy in relation to the spontaneity of chemical processes.

... which translates into:

- electronic structure theory and ways to solve the corresponding equations
- solution of the equations of motion for atoms and electrons + statistical mechanics (from the microcanonical to the canonical ensemble)
- approximate solutions for the description of the interaction with the environment.
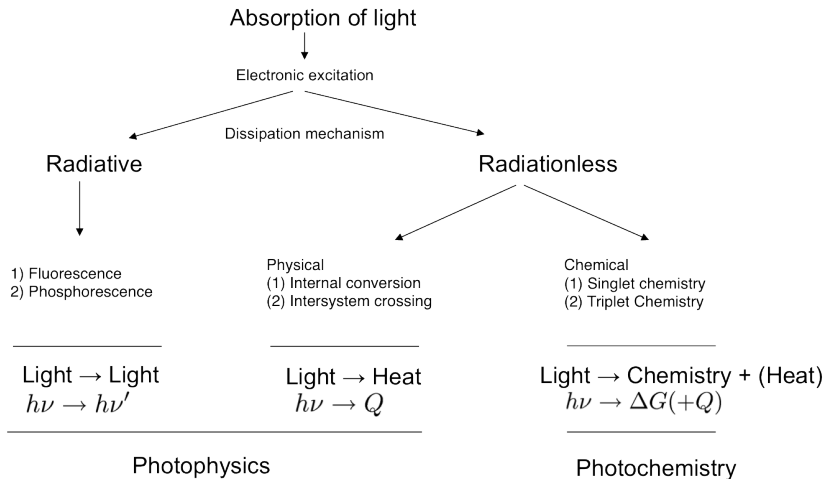
Photochemistry is about atomic rearrangements

From Wikipedia:

Photochemistry, a sub-discipline of chemistry, is the study of the interactions between atoms, small molecules, and light (or electromagnetic radiation). [. . .] Photochemistry may also be introduced to laymen as a reaction that proceeds with the absorption of light. Normally a reaction (not just a photochemical reaction) occurs when a molecule gains the necessary activation energy to undergo change. A simple example can be the combustion of gasoline (a hydrocarbon) into carbon dioxide and water. This is a chemical reaction where one or more molecules/chemical species are converted into others. For this reaction to take place activation energy should be supplied. The activation energy is provided in the form of heat or a spark. In case of photochemical reactions light provides the activation energy.

Interesting there are no entries for **Photophysics** (Jan 2014).

Photochemistry is about atomic rearrangements

Absorption of light

$\downarrow$

Electronic excitation

Dissipation mechanism

Radiative

$\downarrow$

1) Fluorescence
2) Phosphorescence

———————

Light $\rightarrow$ Light
$h\nu \rightarrow h\nu'$

Radiationless

Physical
(1) Internal conversion
(2) Intersystem crossing

Chemical
(1) Singlet chemistry
(2) Triplet Chemistry

———————

Light $\rightarrow$ Heat
$h\nu \rightarrow Q$

———————

Light $\rightarrow$ Chemistry + (Heat)
$h\nu \rightarrow \Delta G(+Q)$

———————

Photophysics

Photochemistry

Why TDDFT in chemistry?

Wavefunction-based methods for excited states properties

Most of the wavefunction-based methods in quantum chemistry are **more** accurate than TDDFT (using the *standard* exchange and correlation functionals) **but** their use is limited to small systems (up to 10-20 atoms).

The ZOO of quantum chemical methods

Wavefunction based methods suited for excited states calc.	SR (single reference = 1 Slater determinant)	MR (multi reference = more than 1 Slater determinant weighted by the coefficients C_i)
CI (Configuration Interaction)	CIS (D) (In bracket extension via perturb)	Full CI CISD, QCISD
CC (coupled-cluster)	CC2 (SRCC with approximated second order corrections)	MRCC CCSD, CCSD(T)
SCF (self-consistent field. Orbitals optimized like in HF)	-	MCRCF CASSCF, CASPT2
MPn (Møller-Plesset)	-	MP2 and MP4

TDDFT for excitation energies of large molecules

Among the single reference (SR) (plus perturbation) methods:

- CIS: is practically no longer used in the calculation of excitation energies in molecules.
  The error in the correlation energy is usually very large and gives qualitatively wrong results.
  STILL good to gain insights into CT states energies.
  Largely replaced by TDDFT.
- CC2: is a quite recent development and therefore not widely available.
  Accurate and fast, is the best alternative to TDDFT.
  Good energies also for CT states.

TDDFT for excitation energies of large molecules

Among the single reference (SR) (plus perturbation) methods:

- CIS: is practically no longer used in the calculation of excitation energies in molecules.
  The error in the correlation energy is usually very large and give qualitatively wrong results.
  STILL good to gain insights into CT state energies.
  Largely replaced by TDDFT.
- CC2: is a quite recent development and therefore not widely available.
  Accurate and fast, is the best alternative to TDDFT.
  Good energies also for CT states.

Multi reference (MR) *ab initio* methods are still computationally too expensive for large systems (they are limited to few tenths of atoms) and for mixed-quantum classical dynamics. However, there are many interesting new developments (MR-CISD, G-MCQDPT2).

TDDFT for excitation energies of large molecules

TDDFT :

- is formally exact and improvements of the xc-functionals are still possible.
- is computationally more efficient and scales better than *ab-initio* wavefunction-based methods.
- can be used for large systems (up to thousand atoms).
- can be easily combined with MD (mixed quantum classical MD)
- **BUT is not a black box !**

TDDFT for excitation energies of large molecules

TDDFT :

- is formally exact and improvements of the xc-functionals are still possible.
- is computationally more efficient and scales better than *ab-initio* wavefunction-based methods.
- can be used for large systems (up to thousand atoms).
- can be easily combined with MD (mixed quantum classical MD)
- **BUT is not a black box !**

Failure of density-functional theory and time-dependent density-functional theory for large extended π systems

Zheng-Li Cai, Karina Sendt, and Jeffrey R. Reimers[a]
School of Chemistry, The University of Sydney, New South Wales, 2006 Australia

TDDFT for excitation energies of large molecules

TDDFT :

- is formally exact and improvements of the xc-functionals are still possible.
- is computationally more efficient and scales better than *ab-initio* wavefunction-based methods.
- can be used for large systems (up to thousand atoms).
- can be easily combined with MD (mixed quantum classical MD)
- **BUT is not a black box !**

**Failure of time-dependent density functional theory for excited state surfaces in case of homolytic bond dissociation**

K.J.H. Giesbertz, E.J. Baerends *

Afdeling Theoretische Chemie, Vrije Universiteit, De Boelelaan 1083, 1081 HV Amsterdam, The Netherlands

TDDFT for excitation energies of large molecules

TDDFT :

- is formally exact and improvements of the xc-functionals are still possible.
- is computationally more efficient and scales better than *ab-initio* wavefunction-based methods.
- can be used for large systems (up to thousand atoms).
- can be easily combined with MD (mixed quantum classical MD)
- **BUT is not a black box !**

J|A|C|S

A R T I C L E S

Published on Web 03/06/2004

Failure of Time-Dependent Density Functional Theory for Long-Range Charge-Transfer Excited States: The Zincbacteriochlorin−Bacteriochlorin and Bacteriochlorophyll−Spheroidene Complexes

Andreas Dreuw[*,†] and Martin Head-Gordon[‡]

TDDFT can easily be combined with molecular dynamics

Ultrafast tautomerization of 4-hydroxyquinoline·$(NH_3)_3$
Hydrogen or proton transfer along this molecular wire?
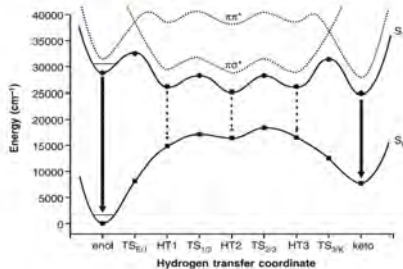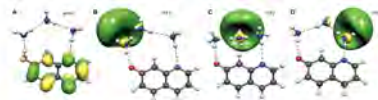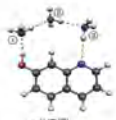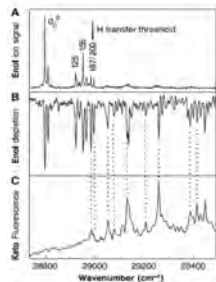
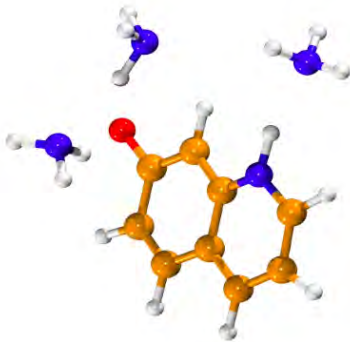CIS/CASSCF for the in-plane geometry $\to$ $\pi\pi^*/\pi\sigma^*$ crossing leads to a hydrogen atom transfer.
S. Leutwyler *et al.*, Science, 302, 1736 (2003)

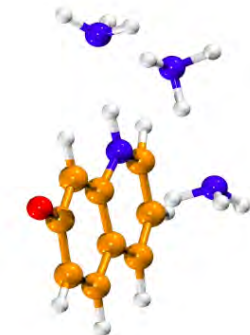# TDDFT can easily be combined with molecular dynamics

Ultrafast tautomerization of 4-hydroxyquinoline·$(NH_3)_3$
Hydrogen or proton transfer along this molecular wire?

What about TDDFT combined with nonadiabatic dynamics?

TDDFT can easily be combined with molecular dynamics

Ultrafast tautomerization of 4-hydroxyquinoline·$(NH_3)_3$
Hydrogen or proton transfer along this molecular wire?

What about TDDFT combined with nonadiabatic dynamics?

TDDFT can easily be combined with molecular dynamics

Ultrafast tautomerization of 4-hydroxyquinoline·$(NH_3)_3$
Hydrogen or proton transfer along this molecular wire?

With TDDFT, we observe:

- Symmetry breaking.
- No crossing with the $\pi\sigma^*$ state.
- Proton transfer instead of a hydrogen transfer.

Guglielmi *et al.*, PCCP, 11, 4549 (2009).

TDDFT can easily be combined with molecular dynamics

Ultrafast tautomerization of 4-hydroxyquinoline$\cdot(NH_3)_3$
Hydrogen or proton transfer along this molecular wire?
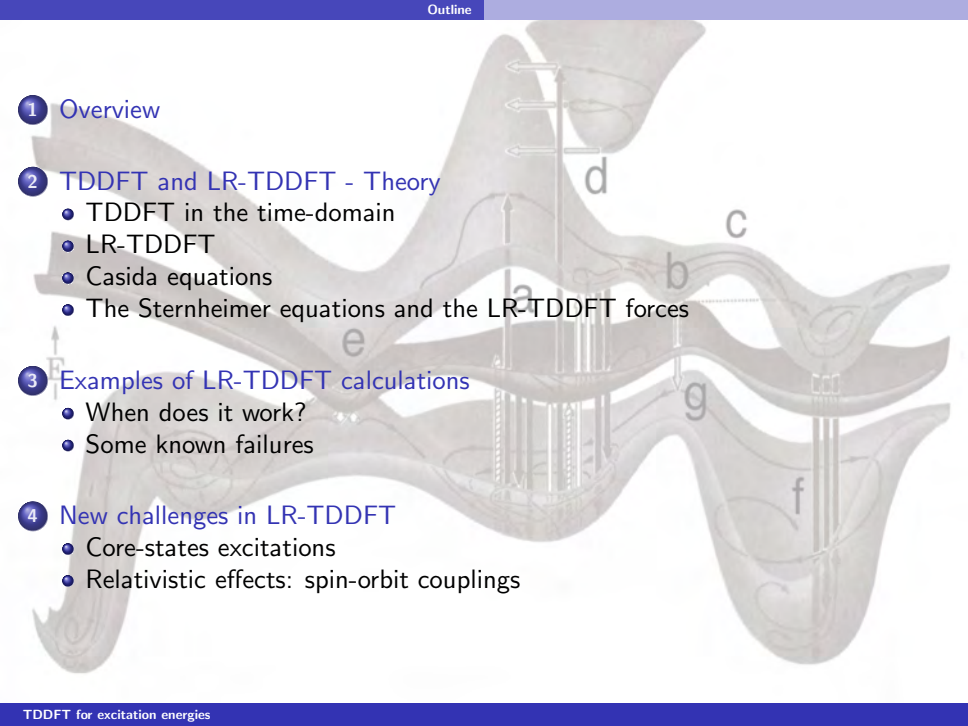Similar observations with CASPT2 calculations:
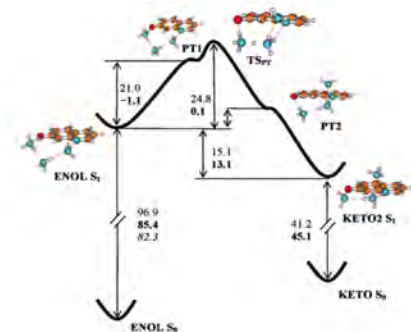
Forcing in-plane symmetry: hydrogen transfer.
Unconstrained geometry optimization leads to a proton transfer!
Fernandez-Ramos *et al.*, JPCA, 111, 5907 (2007).

Main topics of this set of lectures

Topics of this set of lectures

1. Review basic theory of TDDFT and LR-TDDFT.
2. Look at critical failures of current *xc*-functionals.
3. *Ab initio* molecular dynamics.
4. Nonadiabatic dynamics using LR-TDDFT.
5. Coupling with the environment (TDDFT/MM).

The time-dependent KS equations

The role played by the second Hohenberg-Kohn theorem in the derivation of the time-independent DFT equation is now taken by a variational principle involving the action,

$$A[\Psi] = \int_{t_0}^{t_1} \langle \Psi(t)|i\frac{\partial}{\partial t} - \hat{H}(t)|\Psi(t)\rangle dt.$$

The wavefunction is determined up to a time-dependent constant

$$\Psi(\mathbf{r}_1, \ldots, \mathbf{r}_N, t) = \Psi[\rho](t)e^{-i\alpha(t)}$$

The effect of the phase factor is simply to contribute with an additive constant to the total action,

$$\tilde{A}[\rho] = \int_{t_0}^{t_1} \langle \tilde{\Psi}[\rho](t)|i\frac{\partial}{\partial t} - \hat{H}(t)|\tilde{\Psi}[\rho](t)\rangle dt + \alpha(t_1) - \alpha(t_0) = A[\rho] + \text{const.}$$

Thus the time-dependent density determines the action, up to an additive constant.

RG II

The true time-dependent density is the one which makes the action stationary,

$$0 = \frac{\delta A[\rho]}{\delta\rho(\mathbf{r}, t)} = \int_{t_0}^{t_1} \langle \frac{\delta\Psi(t')}{\delta\rho(\mathbf{r}, t)}|i\frac{\partial}{\partial t'} - \hat{H}(t')|\Psi(t')\rangle dt' + c.c. \ .$$

Corrected action density functional: R. van Leeuwen, *Phys. Rev. Lett.*, **80**, 1280 (1998).

The time-dependent KS equations

The functional $A[\rho]$ can be written as

$$A[\rho] = B[\rho] - \int d\mathbf{r} \int_{t_0}^{t_1} dt\, v(\mathbf{r}; \mathbf{R}, t)\rho(\mathbf{r}, t)$$

where the *universal* functional $B[\rho]$ is independent of the external potential.
In analogy with to the time-dependent Kohn-Sham equation, we may assume an
independent particle system whose orbitals $\psi_i(\mathbf{r}, t)$ have the property:

$$\rho(\mathbf{r}, t) = \sum_i f_i |\psi_i(\mathbf{r}, t)|^2$$

Using this definition, we can write $B[\rho]$ as:

$$B[\rho] = \sum_i f_i \int_{t_0}^{t_1} dt \langle \psi_i(t)|i\frac{\partial}{\partial t} - \frac{1}{2}\nabla_i^2|\psi_i(t)\rangle$$

$$- \frac{1}{2} \int_{t_0}^{t_1} dt \int \int d\mathbf{r_1} d\mathbf{r_2} \frac{\rho(\mathbf{r_1}, t)\rho(\mathbf{r_2}, t)}{|\mathbf{r_1} - \mathbf{r_2}|} - \mathcal{A}_{xc}[\rho]$$

where $\mathcal{A}_{xc}[\rho]$ is the exchange and correlation action functional.

The time-dependent KS equations

Applying the variational principle to

$$A[\rho] = B[\rho] - \int d\mathbf{r} \int_{t_0}^{t_1} dt \, v(\mathbf{r}; \mathbf{R}, t)\rho(\mathbf{r}, t)$$

with the constraint that

$$\rho(\mathbf{r}, t) = \sum_i f_i |\psi_i(\mathbf{r}, t)|^2 = \sum_i^N |\psi_i(\mathbf{r}, t)|^2$$

leads to the time-dependent Kohn-Sham equation:

$$\left[-\frac{1}{2}\nabla^2 + v_{\text{eff}}(\mathbf{r}, t) \right] \psi_i(\mathbf{r}, t) = i\frac{\partial}{\partial t}\psi_i(\mathbf{r}, t)$$

$$v_{\text{eff}}(\mathbf{r}, t) = v_{\text{H}}(\mathbf{r}, t) + v_{\text{xc}}(\mathbf{r}, t) + v_{\text{ext}}(\mathbf{r}, t)$$

The unknown is now the time-dependent *xc* potential

$$v_{xc}(\mathbf{r}, t) = \frac{\delta \mathcal{A}_{\text{xc}}[\rho]}{\delta \rho(\mathbf{r}, t)}$$

Adiabatic Approximation in TDDFT

In analogy to the traditional time-independent Kohn-Sham scheme, all exchange and correlation effects in TDDFT are collected into $\delta \mathcal{A}_{xc}[\rho]/\delta \rho(\mathbf{r}, t)$.

In the formal derivation of the time-dependent density functional equations (both the time-dependent KS equations and the linear response matrices) no approximations are made, and therefore the theory is *in principle exact*.

However, the exact time-dependent exchange-correlation action functional is not known, and approximations have to be introduced in order to perform numerical calculations on real systems.

Adiabatic Approximation in TDDFT

Within the adiabatic approximation (AA),

$$v_{xc}[\rho](\mathbf{r}, t) = \frac{\delta \mathcal{A}_{xc}[\rho]}{\delta \rho(\mathbf{r}, t)} \approx \left. \frac{\delta E_{xc}[\rho]}{\delta \rho(\mathbf{r})} \right|_{\rho=\rho(\mathbf{r}, t)}$$

We assume that the exchange and correlation potential changes instantaneously when the electron density is changed! No retardation effects!

we can use all xc functionals, $v_{xc}(\mathbf{r})$, derived for the time-independent DFT also for the time-dependent functionals, $v_{xc}(\mathbf{r})|_t$ and $f_{xc}(\mathbf{r}, \mathbf{r}')|_t$ (including hybrid functionals).

The TDDFT xc-kernel used in the AA becomes

$$f_{xc}^{\sigma\tau}(\mathbf{r}t, \mathbf{r}'t') = \delta(t - t') \frac{\delta^2 E_{xc}[\rho]}{\delta \rho_\sigma(\mathbf{r}) \delta \rho_\tau(\mathbf{r}')}.$$

CAUTION

Important approximation! We neglect all retardation or memory effects!

Real time dynamics in TD Kohn-Sham scheme

$$\left[-\frac{1}{2}\nabla^2 + v_{\text{eff}}(\mathbf{r}, t)\right] \psi_i(\mathbf{r}, t) = i \frac{\partial}{\partial t} \psi_i(\mathbf{r}, t)$$

- Propagation of the time-dependent Kohn-Sham equations:

$$\psi_i(t) = \mathcal{U}(t, t_0) \psi_i(t_0)$$

$$\mathcal{U}(t, t_0) = \hat{T} \exp\left[-i \int_{t_0}^{t} \mathcal{H}_{\text{KS}}(t') \, dt'\right]$$

- Since the real dynamics of the electrons has high frequencies, the time step for propagation is very small ($\sim 10^{-3}$ a.u.)
- Problem: we need to find a good approximations for the time-evolution operator [1].

---

[1] For a very complete discussion, see A. Castro, M. A. L. Marques, and A. Rubio, J Chem Phys 121, 3425-3433 (2004).

Propagators

- **Iterative Chebysheff interpolation scheme**, combined with a two step Runge-Kutta scheme to maintain order Δt^3 accuracy.
  A first guess for the potential at time $t_0 + \Delta t/2$, $v_{eff}(\mathbf{r}, t_0 + \Delta t/2)$, is obtained by evolving the KS states using the effective potential at time t_0. The full time-evolution is then achieved by evolving the wavefunctions for the full time step Δt, using the approximated potential computed from the half step. For a given effective potential $v_{eff}(\mathbf{r}, t)$, the solution of the time-dependent Schrödinger-like equations, for both half and full steps, is accomplished by iterating until convergence the set of integral equations

$$\phi_j^{(n)}(t_0 + \Delta t) = \phi_j^{(0)}(t_0 + \Delta t) - i \int_{t_0}^{t_0 + \Delta t} d\tau \, \hat{\mathcal{H}}_{KS}\big(\{\phi_i^{(n-1)}(\tau)\}, \tau\big) \, \phi_j^{(n-1)}(\tau).$$

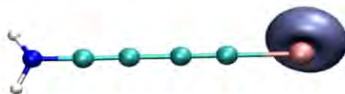 The integrals are computed by Chebyshev interpolation in the time domain.

- The implicit midpoint rule, also known as **Crank-Nicholson** method

$$\hat{U}_{CN}(t + \Delta t, t) = \frac{1 - \frac{i}{2}\Delta t \, \hat{\mathcal{H}}_{KS}(t + \Delta t/2)}{1 + \frac{i}{2}\Delta t \, \hat{\mathcal{H}}_{KS}(t + \Delta t/2)}$$

  The CN scheme is unitary and preserves time-reversal symmetry.

Both schemes are implemented in CPMD.

Example: Time propagation of the electronic density

Electronic spin density dynamics ($\rho_\alpha(\mathbf{r}, t) - \rho_\beta(\mathbf{r}, t)$) dynamics after photoinduced ionization on a simple model compound.
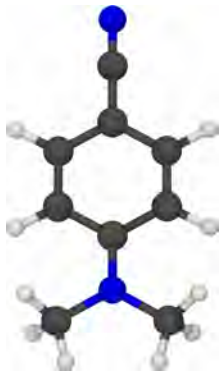
Absorption spectra calculation

N,N-dimethylaminobenzonitrile
(DMABN)

1. Ground state Kohn-Sham calculation.

2. Time propagation of the KS orbitals:
   - Apply a short perturbative field (usually an instantaneous perturbation on the KS orbitals).
   - Propagate the perturbed orbitals for a long time (the longer the simulation, the higher the energy resolution).

3. Sample the dipole moment time series $\mu_x(t)$

4. Fourier transform to obtain the dynamic polarizability $\alpha_{xz}(\omega)$ [a].

5. Spectrum can be obtained from the optical absorption cross-section:

$$\sigma(\omega) = \frac{4\pi\omega}{c}\Im\{\alpha(\omega)\}$$

---

[a] more will come soon on this topic...

Absorption spectra calculation

N,N-dimethylaminobenzonitrile
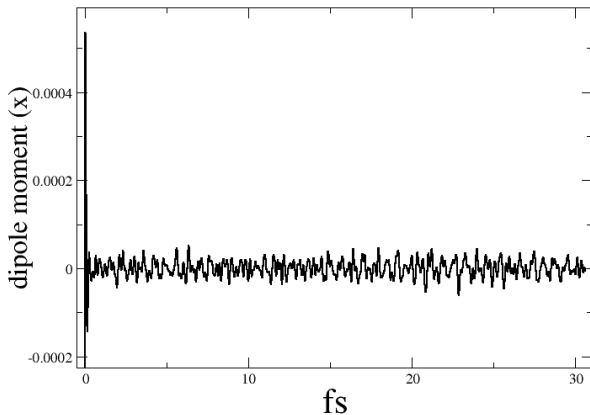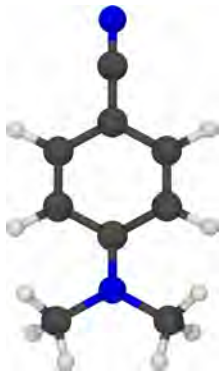(DMABN)

Figure: Dipole moment in the x-direction: $\mu_x(t)$

Absorption spectra calculation
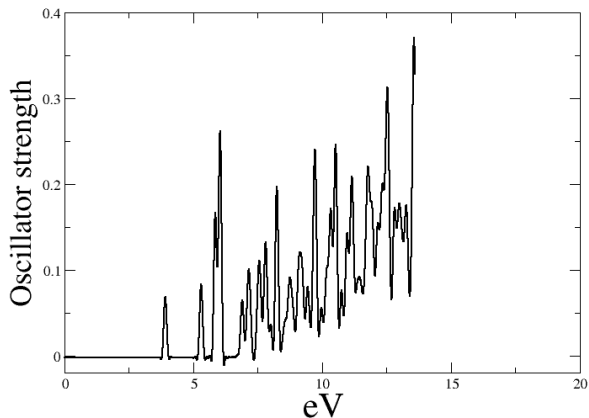

N,N-dimethylaminobenzonitrile
(DMABN)

Figure: Extraction of the absorption spectrum.
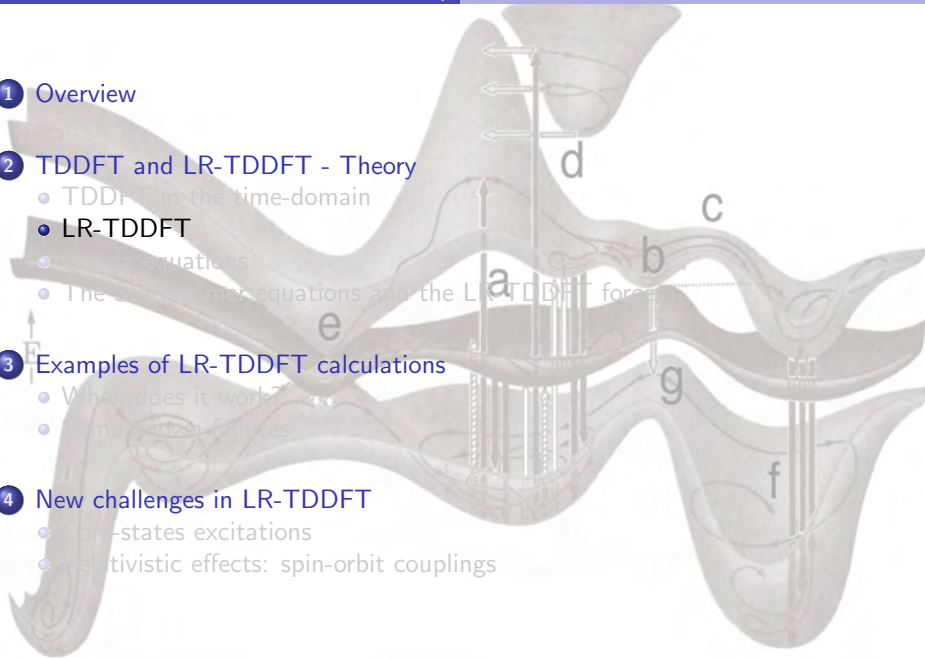
Linear response in TD Kohn–Sham scheme

Linear response time-dependent density functional theory (LR-TDDFT); The chemists prospective

Different solutions:

- Mark E. Casida, *Time-Dependent Density Functional Response Theory for Molecules*, in *"Recent advances in Density Functional Theory"*, ed. D.P. Chong, Singapore, World Scientific (1995), p155.

- *Molecular excitation energies from time-dependent density functional theory*, T. Grabo, M. Petersilka, & E.K.U. Gross, *THEO CHEM* **501-502**, 353-367 (2000)

- The Sternheimer time-dependent perturbation scheme. See for instance *Excited state nuclear forces from the Tamm–Dancoff approximation to time-dependent density functional theory within the plane wave basis set framework*, Jürg Hutter, JPC (2003)

Time-Dependent Density Functional Response Theory (LR-TDDFT).

In the linear response formulation of TDDFT (LR-TDDFT) one studies the density response of a system under the influence of an external time dependent perturbation,

$$\rho(\mathbf{r}, t) = \rho_0(\mathbf{r}) + \delta\rho(\mathbf{r}, t)$$

The basic quantity in the LR-TDDFT is the density-density response function

$$\chi(\mathbf{r}, t, \mathbf{r}', t') = \frac{\delta\rho(\mathbf{r}, t)}{\delta v_{ext}(\mathbf{r}', t')}\bigg|_{v_0}$$

which relates the first order density response $\delta\rho(\mathbf{r}, t)$ to the applied perturbation $\delta v(\mathbf{r}, t)$

$$\delta\rho(\mathbf{r}, t) = \int_{t_0}^{t} dt' \int d\mathbf{r}' \, \delta v(\mathbf{r}', t') \, \chi(\mathbf{r}, t, \mathbf{r}', t'),$$

where the total external potential, $v_{ext}(\mathbf{r}, t)$ is given by the sum of the static ground state KS potential, $v_0(\mathbf{r})$, and the external potential $\delta v(\mathbf{r}, t)$.

LR-TDDFT in Physics and Chemistry

There are different ways to represent "*quasi-particles*" states in many-body systems

- Bloch functions
- Wannier functions
- Hartree-Fock orbitals
- Kohn-Sham orbitals

$\triangleright$ Molecular systems are not translational invariant and therefore the momenta are not good quantum numbers. [We cannot FT $(\mathbf{r}_1 - \mathbf{r}_2)$]

$\triangleright$ HF and KS orbitals constitute a discrete basis of one-electron states $\{\phi_i(\mathbf{r})\}$ for the expansion of all many-body operators.

$\triangleright$ In chemistry the LR-TDDFT equations are expressed in matrix form using the Kohn-Sham base.

Time-Dependent Density Functional Response Theory (LR-TDDFT).

The first order density response $\delta\rho(\mathbf{r}, t)$ can be expanded in the basis of unperturbed orbitals $\{\phi_i\}$

$$
\begin{aligned}
\delta\rho(\mathbf{r}, t) &= \int_{t_0}^{t} dt' \int d\mathbf{r}' \, \delta v(\mathbf{r}', t') \, \chi(\mathbf{r}, t, \mathbf{r}', t') \\
&= \sum_{ijkl} \int_{t_0}^{t} dt' \int d\mathbf{r}' \, \delta v(\mathbf{r}', t') \, \left(\phi_i^*(\mathbf{r})\phi_j(\mathbf{r})\phi_k^*(\mathbf{r}')\phi_l(\mathbf{r}')\chi_{ij,kl}(\mathbf{r}, t, \mathbf{r}', t') \right) \\
&= \sum_{ijkl} \int_{t_0}^{t} dt' \left(\int d\mathbf{r}' \, \delta v(\mathbf{r}', t') \, \phi_k^*(\mathbf{r}')\phi_l(\mathbf{r}') \right) \phi_i^*(\mathbf{r})\phi_j(\mathbf{r})\chi_{ij,kl}(\mathbf{r}, t, \mathbf{r}', t') \\
&= \sum_{ijkl} \int_{t_0}^{t} dt' \, \delta v_{kl}(t')\phi_i^*(\mathbf{r})\phi_j(\mathbf{r})\chi_{ij,kl}(\mathbf{r}, t, \mathbf{r}', t') \\
&= \sum_{ij} \left(\int_{t_0}^{t} dt' \sum_{kl} \delta v_{kl}(t')\chi_{ij,kl}(\mathbf{r}, t, \mathbf{r}', t') \right) \phi_i^*(\mathbf{r})\phi_j(\mathbf{r}) \\
&= \sum_{ij} \delta P_{ij}(t)\phi_i^*(\mathbf{r})\phi_j(\mathbf{r})
\end{aligned}
$$

Time-Dependent Density Functional Response Theory (LR-TDDFT).

Expressed in matrix form, the linear response of the electronic density is

$$\delta P_{ij}(t) = \int_{t_0}^{t} dt' \sum_{kl} \delta v_{kl}(t') \chi_{ij,kl}(\mathbf{r}, t, \mathbf{r}', t')$$

In Fourier space,

$$\delta \tilde{P}_{ij}(\omega) = \sum_{kl} \delta v_{kl}(\omega) \chi_{ij,kl}(\omega)$$

Where

$$\chi(r, r', t - t') = \Pi^R(r, r', t - t')$$

$$i\Pi(r, r', t - t') = \langle \Psi_0 | T[\hat{\psi}_H^\dagger(r, t)\hat{\psi}_H(r, t)\hat{\psi}_H^\dagger(r', t')\hat{\psi}_H(r', t')] | \Psi_0 \rangle$$
$$= \sum_{ij, kl} \phi_i^*(r)\phi_j(r)\phi_k^*(r')\phi_l(r') \Pi_{ij,kl}(t - t')$$

and

$$i\Pi_{ij,kl}(t - t') = \langle \Psi_0 | T[\hat{a}_{Hi}^\dagger(t)\hat{a}_{Hj}(t)\hat{a}_{Hk}(t')^\dagger \hat{a}_{Hl}(t')] | \Psi_0 \rangle$$

Linear response TDDFT

The response function for the physical system of interacting electrons, $\chi(\mathbf{r}, t, \mathbf{r}', t')$, can be computed from the Dyson-like equation
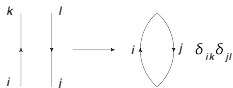
$$\chi(\mathbf{r}, t, \mathbf{r}', t') = \chi_s(\mathbf{r}, t, \mathbf{r}', t') +$$

$$+ \int d\mathbf{r}_1 dt_1 \int d\mathbf{r}_2 dt_2 \, \chi_s(\mathbf{r}, t, \mathbf{r}_1, t_1) \left(\frac{\delta(t_1 - t_2)}{|\mathbf{r}_1 - \mathbf{r}_2|} + \frac{\delta v_{xc}(\mathbf{r}_1, t_1)}{\delta\rho(\mathbf{r}_2, t_2)} \right) \chi(\mathbf{r}_2, t_2, \mathbf{r}, t_1),$$

whre $\chi_s(\mathbf{r}, t, \mathbf{r}', t')$ is the "non interacting" density response

$$\chi_s(\mathbf{r}, \mathbf{r}', \omega) = \sum_{k,j} (f_k - f_j) \frac{\psi_k^*(r)\psi_j(r)\psi_j(r')\psi_k^*(r')}{\omega - (\epsilon_j - \epsilon_k) + i\eta}$$

(η is a positive infinitesimal)

For $\chi_s(\mathbf{r}, \mathbf{r}', \omega)$ evaluate

$g_{ik}^0(\omega)$ is the Fourier transform of the single-electron propagator

$$g_{ik}^0(\omega) = \delta_{ik} \left[\frac{f_i}{\omega - \epsilon_i + i\eta} + \frac{(1 - f_i)}{\omega - \epsilon_i - i\eta} \right]$$

Linear response TDDFT

The relationship between the exact density response function and the Kohn-Sham response function, is compactly expressed in term of the inverse of their corresponding Fourier transform the time, $t_2 - t_1$,

$$\chi^{-1}(\mathbf{r}, \mathbf{r}', \omega) = \chi_s^{-1}(\mathbf{r}, \mathbf{r}', \omega) - \frac{1}{|\mathbf{r}_1 - \mathbf{r}_2|} - f_{xc}(\mathbf{r}_1, \mathbf{r}_2, \omega)$$

In summary, the problem of finding excitation energies of the interacting system has been mapped into the search for the poles of the response function.

$$\{\omega_I, f_I\} \Rightarrow \text{ poles of } \chi(\omega)$$

In fact, $\chi(\omega)$ has poles at the true excitation energies ω_I, while the non-interacting response, $\chi_s(\omega)$, has poles at the Kohn-Sham orbital energy differences.

Linear response TDDFT in molecular spectroscopy

Of particular interest in molecular spectroscopy is the computation of the dynamic dipole polarizability, $\alpha(\omega)$, which is the response function that relates the external potential to the change in the dipole (without loss of generality we consider the effect on the x-component of the dipole induced by an electric field polarized in the z-direction).

$$\mu_x(t) = \mu_x(t_0) + \int_{-\infty}^{\infty} dt' \alpha_{xz}(t - t') \mathcal{E}_z(t') + ...$$

Using the convolution theorem

$$f(t) = \int_{-\infty}^{\infty} dt' g(t - t') h(t') \Longrightarrow f(\omega) = g(\omega) h(\omega)$$

The Fourier transform of the dynamic dipole polarizability can be written as

$$\delta\mu_x(\omega) = \alpha_{xz}(\omega)\, \mathcal{E}_z(\omega)$$

Linear response TDDFT in molecular spectroscopy

$$\delta\mu_x(\omega) = \alpha_{xz}(\omega)\,\mathcal{E}_z(\omega)$$

Using the previously derived expression

$$\delta\tilde{P}_{ij}(\omega) = \sum_{kl}\delta v_{kl}(\omega)\chi_{ij,kl}(\omega)$$

and knowing the definition:

$$\delta\mu_x(\omega) = -\sum_{ij}x_{ij}\delta\tilde{P}_{ij}(\omega) = -\sum_{ijkl}x_{ij}\delta v_{kl}(\omega)\chi_{ij,kl}(\omega)$$

$$= -\sum_{ijkl}x_{ij}\mathcal{E}_z(\omega)z_{kl}\chi_{ij,kl}(\omega)\,,$$

we obtain:

$$\alpha_{xz}(\omega) = \frac{\delta\mu_x(\omega)}{\mathcal{E}_z(\omega)} = -\sum_{ijkl}x_{ij}\chi_{ij,kl}(\omega)z_{kl}\,.$$

$(x_{ij} = \langle\psi_j|\hat{x}|\psi_j\rangle)$.

Linear response TDDFT in molecular spectroscopy

According to the sum-over-states (SOS) relation,

$$\overline{\alpha}(\omega) = \sum_I \frac{f_I}{\omega_I^2 - \omega^2}$$

and considering that

$$f_I = \frac{2}{3}\omega_I(|\langle\Psi_0|\hat{x}|\Psi_I\rangle|^2 + |\langle\Psi_0|\hat{y}|\Psi_I\rangle|^2 + |\langle\Psi_0|\hat{z}|\Psi_I\rangle|^2)$$

and

$$\omega_I = E_I - E_0$$

the poles of the dynamic polarizability determine the excitation energies, ω_I, while the residues, f_I, determine the corresponding oscillator strengths.

$$\alpha_{xz}(\omega) = \frac{\delta\mu_x(\omega)}{\mathcal{E}_z(\omega)} = -\sum_{ijkl} x_{ij}\chi_{ij,kl}(\omega)z_{kl} \, .$$

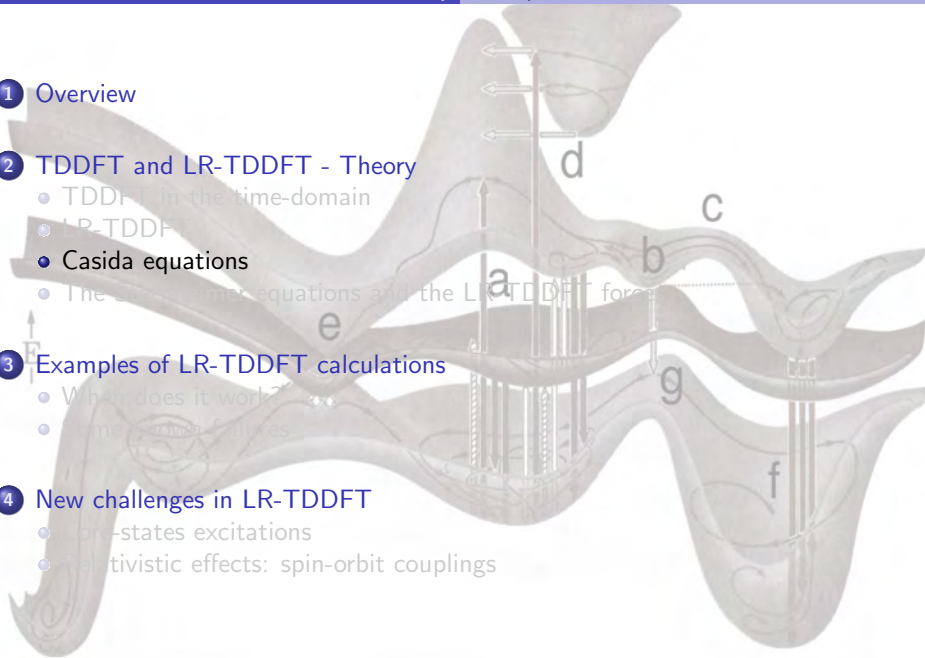**1** Overview

2 TDDFT and LR-TDDFT - Theory
- TDDFT in the time-domain
- LR-TDDFT
- Casida equations
- The Sternheimer equations and the LR-TDDFT forces

3 Examples of LR-TDDFT calculations
- When does it work?
- Numerical failures

4 New challenges in LR-TDDFT
- Spin-states excitations
- Relativistic effects: spin-orbit couplings

The Casida equations

By expressing the dynamic polarizability in the basis of unperturbed MOs, Casida showed that the TDDFT excitation energies

$$\chi^{-1}(\mathbf{r}, \mathbf{r}', \omega) = \chi_s^{-1}(\mathbf{r}, \mathbf{r}', \omega) - \frac{1}{|\mathbf{r}_1 - \mathbf{r}_2|} - f_{xc}(\mathbf{r}_1, \mathbf{r}_2, \omega)$$

are solutions of the system of equations

$$\left[\begin{array}{cc} \mathbf{A}(\omega) & \mathbf{B}(\omega) \\ \mathbf{B}^*(\omega) & \mathbf{A}^*(\omega) \end{array} \right] \left[\begin{array}{c} \vec{X}_I \\ \vec{Y}_I \end{array} \right] = \omega_I \left[\begin{array}{cc} \mathbf{1} & \mathbf{0} \\ \mathbf{0} & -\mathbf{1} \end{array} \right] \left[\begin{array}{c} \vec{X}_I \\ \vec{Y}_I \end{array} \right].$$

Here

$$A_{ia\sigma,jb\tau}(\omega) = \delta_{\sigma\tau}\delta_{ij}\delta_{ab}(\epsilon_{a\sigma} - \epsilon_{i\sigma}) + (ia|f_H + f_{xc}^{\sigma\tau}(\omega)|jb)$$

$$B_{ia\sigma,jb\tau}(\omega) = (ia|f_H + f_{xc}^{\sigma\tau}(\omega)|bj),$$

where

$$f_{xc}^{\sigma\tau}(\mathbf{r}_1, \mathbf{r}_2; \omega) = \int_{-\infty}^{+\infty} e^{i\omega(t_1 - t_2)} \frac{\delta^2 \mathcal{A}_{xc}[\rho_\uparrow, \rho_\downarrow]}{\delta\rho_\sigma(\mathbf{r}_1, t_1)\delta\rho_\tau(\mathbf{r}_2, t_2)} d(t_1 - t_2).$$

The Casida equations - adiabatic case

In the AA Casida's equations simplify to

$$
\begin{bmatrix} \mathbf{A} & \mathbf{B} \\ \mathbf{B}^* & \mathbf{A}^* \end{bmatrix}
\begin{bmatrix} \vec{X}_I \\ \vec{Y}_I \end{bmatrix} = \omega_I
\begin{bmatrix} \mathbf{1} & \mathbf{0} \\ \mathbf{0} & -\mathbf{1} \end{bmatrix}
\begin{bmatrix} \vec{X}_I \\ \vec{Y}_I \end{bmatrix}.
$$

Where

$$
A_{ia\sigma,jb\tau} = \delta_{\sigma\tau}\delta_{ij}\delta_{ab}(\epsilon_{a\sigma} - \epsilon_{i\sigma}) + (ia|f_H + f_{xc}^{\sigma\tau}|jb)
$$

$$
B_{ia\sigma,jb\tau} = (ia|f_H + f_{xc}^{\sigma\tau}|bj),
$$

and

$$
f_{xc}^{\sigma\tau}(\mathbf{r}_1, \mathbf{r}_2) = \frac{\delta^2 E_{xc}[\rho]}{\delta\rho_\sigma(\mathbf{r}_1)\delta\rho_\sigma(\mathbf{r}_2)}
$$

Note that the frequency dependence of the matrices **A** and **B** drops.

Adiabatic Approximation in LR-TDDFT

Since also f_{xc} becomes frequency independent, the number of solutions of the LR-TDDFT equations is just equal to the dimensions of Casida's matrices.

This corresponds exactly to the number of possible one-electron excitations in the system. Hence we conclude that, although the AA does include important correlations effects, it is essentially a one-electron (CIS-like) theory.

LR-TDDFT within the AA has become the most widely used implementation of TDDFT. This theory is known to work well for low-lying excitations of primarily single electron character, which do not involve too large charge density relaxations and which are at least somewhat localized in space.

Caution

Notation: **AA** or **ALDA** are both used. Sometimes, **ALDA** means that, in addition to AA, LDA functional is used for the *xc*-kernel.

Tamm-Dancoff approximation (TDA)

The TDA consists of setting $\mathbf{B} = 0$ in Casida equation. We obtain:

$$\mathbf{A}\vec{X}_I = \omega_I \vec{X}_I$$

which is comparable to the CIS equation (TDA on the TDHF equations), with the difference that in LR-TDDFT the elements of the matrix $\mathbf{A}$ depend on the exchange-correlation kernel.

Physically, setting $\mathbf{B} = 0$ means neglecting all contributions to the excitation energies coming from the de-excitation of the correlated ground state. Even though an approximation, the TDA can improve the stability of the TDDFT calculations with most of the standard (approximated) functionals. In particular, decoupling the DFT ground state problem from the calculation of the LR-TDDFT excitation energies, TDA can provide better PESs especially in the regions of strong coupling with the ground state. This is of crucial importance for all nonadiabatic MD schemes based on LR-TDDFT PESs.

Summary: LR-TDDFT equations in Casida's form

1. Do a ground state Kohn-Sham calculation: obtain $\{\phi_i\}$ and the corresponding $\{\epsilon_i\}$.

2. Form the matrices **A** (and **B** if TDA is not used).

3. Diagonalize the full matrices or used specific algorithm to extract the first roots: obtain $\{\omega_I\}$ and f_I.

4. Informations about the character of the excited states can be obtained from the vectors $\mathbf{X}_I$ and $\mathbf{Y}_I$ (interpretation).

The Sternheimer equations

Notation:

The KS equations are defined as

$$H_{KS}^{\sigma}|\phi_{i\sigma}^0\rangle = \sum_{j=1}^{N^\sigma} \epsilon_{ij\sigma}|\phi_{j\sigma}^0\rangle$$

with

$$H_{KS}^{\sigma}(r) = -\frac{1}{2}\nabla^2 + V_{SCF}^{\sigma}(r)$$

and ϵ the matrix of Lagrange multipliers

$$\epsilon_{ij\sigma} = \langle\phi_{i\sigma}^0|H_{KS}^{\sigma}|\phi_{j\sigma}^0\rangle\,.$$

The ground state density becomes

$$\rho_{\sigma}^0(r) = \sum_{i=1}^{N^\sigma} \phi_{i\sigma}^{0*}(r)\phi_{i\sigma}^0(r)$$

The Sternheimer equations

We define the perturbing potential as

$$\lambda \delta v(\mathbf{r}, t) = \lambda \delta v^+(\mathbf{r}) e^{i\omega t} + \lambda \delta v^-(\mathbf{r}) e^{-i\omega t}$$

for which

$$\phi_{j\sigma}(\mathbf{r}, t) = e^{-i\varepsilon_j t} \sum_{m=0} \lambda^m \phi_{j\sigma}^{(m)}(\mathbf{r}, t)$$

In first order, $m = 1$, (and setting $\lambda = 1$)

$$\phi_{j\sigma}^{(1)}(\mathbf{r}, t) = \phi_{j\sigma}^{\{+\}}(\mathbf{r}) e^{i\omega t} + \phi_{j\sigma}^{\{-\}}(\mathbf{r}) e^{-i\omega t}$$

from which

$$\rho^{(1)}(\mathbf{r}, t) = \rho^+(\mathbf{r}) e^{i\omega t} + \rho^-(\mathbf{r}) e^{-i\omega t}$$

with

$$\rho^\pm(\mathbf{r}) = \sum_{j\sigma} \phi_{j\sigma}^{\pm *}(r) \phi_{j\sigma}^0(\mathbf{r}) + \phi_{j\sigma}^{0*}(r) \phi_{j\sigma}^\pm(\mathbf{r})$$

The Sternheimer equations

The perturbing potential induces the effective potential energy change

$$\delta v_{\text{eff}}^{\pm}(\mathbf{r}, t) = \delta v^{\pm}(\mathbf{r})e^{\pm i\omega t} + \delta v_{SCF}^{\pm}(\mathbf{r})e^{\pm i\omega t}$$

with

$$\delta v_{SCF}^{\sigma\pm}(\mathbf{r}) = \sum_{\tau \in \{\alpha, \beta\}} \int d^3r' \left(\frac{1}{|\mathbf{r} - \mathbf{r}'|} + \frac{\delta^2 E_{xc}}{\delta\rho_\sigma(\mathbf{r}) \, \delta\rho_\tau(\mathbf{r}')}\Big|_{\rho=\rho^{\{0\}}} \right) \delta\rho_\tau^{\pm}(\mathbf{r}')$$

Until now the frequency ω is still arbitrary.
Inserting into the time-dependent KS equation and keeping only $\mathcal{O}(\lambda)$ one gets

$$\sum_{j=1}^{N^\sigma}(\epsilon_{ij} - (H_{KS}^\sigma\delta_{ij} \pm \omega)\delta_{ij})|\phi_{j\sigma}^{(\pm)}\rangle = \mathcal{Q}_c^\sigma \left(\delta V^\pm + \delta V_{SCF}^\sigma(\pm\omega)\right)|\phi_{i\sigma}^{(0)}\rangle$$

where the response orbitals are chosen perpendicular to the occupied Kohn-Sham states, $|\phi_{i\sigma}^{(0)}\rangle$, $\langle\phi_{i\sigma}^{(\pm)}|\phi_{j\sigma}^{(0)}\rangle = 0$, and $\mathcal{Q}_c^\sigma = \mathbf{1} - \sum_{i=1}^{\text{occ}} |\phi_{i\sigma}^0\rangle\langle\phi_{i\sigma}^0|$.

The Sternheimer equations

The Sternheimer equation is in the form

$$(\mathcal{A} - \omega\mathcal{B})\delta\rho(\omega) = \delta v(\omega)$$

and therefore $\chi^{-1}(\omega) \equiv (\mathcal{A} - \omega\mathcal{B})$.

The resonant energies are therefore computed from the solution of the generalized eigenvalue problem $\chi^{-1}(\omega) = 0$

$$\sum_{j=1}^{\text{occ}} (H_{KS}^{\sigma}\delta_{ij} - \epsilon_{ij\sigma})|\phi_{j\sigma}^{(\pm)}\rangle + \mathcal{Q}_c^{\sigma}\,\delta V_{SCF}^{\sigma}|\phi_{i\sigma}^{(0)}\rangle = \mp\omega|\phi_{i\sigma}^{(\pm)}\rangle$$

Solution strategy:

1. Solve the unperturbed KS equation and get $|\phi_{i\sigma}^{\{0\}}\rangle$

2. Solve the Self-Consistent Sternheimer equations for

   ▸ the excitation energies ω_I
   ▸ the linear response orbitals $|\phi_{i\sigma,I}^{(\pm)}\rangle$
     (the index I labels the different solutions)

The Sternheimer equations

Properties of the Sternheimer approach

- The evaluation of the Sternheimer equations requires only occupied KS orbitals, $\phi_{i\sigma}(r)$: this is an important advantage compared to Casida equations.
- The unoccupied space is only referenced through the projector Q_c^σ.
- The KS orbitals do not have to be in canonical form: no diagonalization of H_{KS}^σ required
- Virtual KS states are only computed for the assignments of the excitations (if required).

The Sternheimer equations: the matrix form

Expanding the ground state KS orbitals and the linear response orbitals in an orthogonal basis set $\{\kappa_p(\mathbf{r})\}$ defines the expansion coefficients $\{c_{pi\sigma}^{\{0\}}\}$ and $\{c_{pi\sigma}^{\{\pm\}}\}$

$$\phi_{i\sigma}^{\{0\}}(\mathbf{r}) = \sum_{p=1}^{M} c_{pi\sigma}^{\{0\}} \kappa_p(\mathbf{r})$$

$$\phi_{i\sigma}^{\{\pm\}}(\mathbf{r}) = \sum_{p=1}^{M} c_{pi\sigma}^{\{\pm\}} \kappa_p(\mathbf{r})$$

In the following, the indices $i, j, k, \ldots$ run over the KS states $(1, \ldots, N_\sigma)$, and the indices $p, q, r, \ldots$ refer to the basis functions $(1, \ldots, M)$.
Introducing the new set of coefficients

$$x_{pi} = \frac{1}{2}(c_{pi}^{\{+\}} + c_{pi}^{\{-\}})$$

$$y_{pi} = \frac{1}{2}(c_{pi}^{\{+\}} - c_{pi}^{\{-\}})$$

For a real perturbation: $\delta\rho^\sigma(+\omega) = \delta\rho^\sigma(-\omega)$ and $\delta V_{SCF}^\sigma(+\omega) = V_{SCF}^\sigma(-\omega)$

The Sternheimer equations: the matrix form

Matrix form of the Sternheimer equations

$$\mathcal{A}(\mathcal{A} + \mathcal{B})\mathbf{x} = \omega^2 \mathbf{x}$$
$$(\mathcal{A} + \mathcal{B})\mathcal{A}\mathbf{y} = \omega^2 \mathbf{y}$$

The (super-) operators $\mathcal{A}$ and $\mathcal{B}$ are defined as ($H = H_{KS}$)

$$\mathcal{A}_{pi\sigma,qj\tau} = \big((H)_{pq\sigma}\delta_{ij} - \epsilon_{ij\sigma}\delta_{pq}\big)\delta_{\sigma\tau}$$
$$\mathcal{B}_{pi\sigma,qj\tau} = \sum_{rst} Q_{tp\sigma} c_{ir\sigma}^{\{0\}} (c_{js\tau}^{\{0\}})^* \mathcal{K}_{tr\sigma,qs\tau}$$

where

$$\mathbf{H}_{pq\sigma} = \langle \kappa_p | H^\sigma | \kappa_q \rangle , \quad \epsilon_{ij} = \sum_{pq} (c_{ip\sigma}^{\{0\}})^* \mathbf{H}_{pq\sigma} c_{jq\sigma}^{\{0\}}$$

$$\mathbf{P}_{pq\sigma} = \sum_i (c_{ip\sigma}^{\{0\}})^* c_{iq\sigma}^{\{0\}} , \quad \mathbf{Q}_{pq\sigma} = \delta_{pq} - \mathbf{P}_{pq\sigma} , \quad \mathbf{W}_{pq\sigma} = \langle \kappa_p | \delta V_{SCF}^\sigma | \kappa_q \rangle$$

$$\mathcal{K}_{tr\sigma,qs\tau} = \int d^3r \int d^3r' \, \kappa_t^*(\mathbf{r})\kappa_r(\mathbf{r})\left[\frac{1}{|\mathbf{r} - \mathbf{r}'|} + \frac{\delta^2 E_{xc}}{\delta\rho_\sigma(\mathbf{r})\delta\rho_\tau(\mathbf{r}')}\Big|_{\rho^{\{0\}}} \right]\kappa_q^*(\mathbf{r}')\kappa_s(\mathbf{r}')$$

LR-TDDFT forces

Analytic derivatives

$$\frac{dE_{tot}[c^{\{0\}}, x, y]}{d\eta} = \frac{dE_{KS}[c^{\{0\}}]}{d\eta} + \frac{d\omega[c^{\{0\}}, x, y]}{d\eta}$$

where η is an external parameter.

A staightforward calculation of $d\omega[c^{\{0\}}, x]/d\eta$ requires derivatives of the MO coefficients which are computationally very costly.
(Especially when η represents the f nuclear degrees of freedom AND we are using atom-centered basis functions!)

strategy

Derive an extended Lagrangian that is vatiational with respect to $c^{\{0\}}$ and x, y in order to eliminate the derivatives of the MO coefficients.
Ref: Sternheimer-Dalgarno interchange theorem: R.M. Sternheimer, H. M. Flory, Phys.Rev. 92, 1460 (1953); S. Dalgarno, Proc. R. Soc. London, Ser. A, 247, 243 (1958).

LR-TDDFT forces: the extended Lagrangian formalism

The TDDFT forces can be derived in a compact way using the Lagrangian formalism.

In the Tamm-Dancoff approximation to the TDDFT equations, the linear response amplitudes, $c^{\{+\}}$, are set to zero and the Sterhheimer equation becomes ($\mathbf{x}_\mu = -\mathbf{y}_\mu$)

$$(\mathcal{A} + \mathcal{B})\,\mathbf{x} = \omega\mathbf{x}$$

The LR-TDDFT/TDA Hermitian eigenvalue equation is related to the extended energy functional

$$\mathcal{L}_{TDA}[c^{\{0\}}, x, \omega] = \mathbf{x}^\dagger(\mathcal{A} + \mathcal{B})\mathbf{x} - \omega(\mathbf{x}^\dagger\mathbf{x} - 1)$$

- $\mathcal{L}_{TDA}[c^{\{0\}}, x, \omega]$ is variational in x and ω.
- we have the following stationary conditions:

$$\frac{\delta\mathcal{L}_{LDA}}{\delta x^\dagger} = (\mathcal{A} + \mathcal{B})\mathbf{x} - \omega\mathbf{x} = 0$$

$$\frac{\delta\mathcal{L}_{LDA}}{\delta\omega} = \mathbf{x}\mathbf{x}^\dagger - 1 = 0$$

LR-TDDFT forces: the extended Lagrangian formalism

The extended Lagrangian functional that is variational in all wavefunction coefficients $c^{\{0\}}, x$ is

$$\mathcal{L}_{tot}[c^{\{0\}}, x, \omega, \Lambda, Z] =$$
$$= \mathcal{L}_{KS}[c^{\{0\}}, \Lambda] + \mathcal{L}_{TDA}[c^{\{0\}}, x, \omega] + \sum_{pi\sigma} \mathbf{Z}_{pi\sigma} \left\{ \sum_q \mathbf{H}_{pq\sigma} c^{\{0\}}_{qi\sigma} - \sum_j c^{\{0\}}_{qj\sigma} \Lambda_{ji\sigma} \right\}$$

where

$$\mathcal{L}_{KS}[c^{\{0\}}, \Lambda] = E_{KS}[c^{\{0\}}] - \sum_{ij\sigma} \Lambda_{ij\sigma} \left\{ \sum_p (c^{\{0\}}_{pi\sigma})^* c^{\{0\}}_{pj\sigma} - \delta_{ij} \right\}$$
$$\mathcal{L}_{TDA}[c^{\{0\}}, \mathbf{x}, \omega] = \mathbf{x}^\dagger (\mathcal{A} + \mathcal{B}) \mathbf{x} - \omega (\mathbf{x}^\dagger \mathbf{x} - 1)$$

and $\mathbf{Z}$ is the matrix od Lagrangian multipliers associated with the stationarity of the Kohn-Sham orbitals.

LR-TDDFT forces: the extended Lagrangian formalism

Properties of the total extended Lagrangian (within the TDA):

- $\mathcal{L}_{tot}[c^{\{0\}}, x, \omega, \Lambda, Z]$ is required to be stationary with respect to all its variables, $c^{\{0\}}, x, \omega, \Lambda, Z$.

- variation with respect to ω and x give the LR-TDDFT/TDA equations.

- variation with respect to **Z** enforce the ground state KS equations and the MO orthogonality.

- thanks to the variational principle, the *implicit* dependence of $\mathcal{L}_{tot}$ through the MO coefficients drops:
$$\sum_{c^{\{0\}}} \frac{\partial \mathcal{L}}{\partial c^{\{0\}}} \frac{\partial c^{\{0\}}}{\partial \eta} = 0$$

- $\mathcal{L}_{tot}$ depends only from the *explicit* dependence on the external parameter η. We can place the total derivatives $\frac{\partial \mathcal{L}}{\partial \eta} = \mathcal{L}^{\eta}$ with the "explicit" one $\mathcal{L}^{(\eta)}$.

TLR-TDDFT forces: the extended Lagrangian formalism

Considering η as a nuclear displacement

$$\omega^{(\eta)} = \sum_{pi\sigma} \sum_{qj\tau} (x_{pi\sigma})^* \mathcal{A}^{(\eta)} x_{qj\tau} + \sum_{pqi\sigma} Z_{pi\sigma} H^{(\eta)}_{pq\sigma} c^{\{0\}}_{qi\sigma}$$

$$= \sum_{pqi\sigma} (x_{pi\sigma})^* H^{(\eta)}_{pq\sigma} x_{qi\sigma} - \sum_{pji\sigma} \sum_{uv} (x_{pi\sigma})^* (c^{\{0\}}_{ui\sigma})^* H^{(\eta)}_{uv\sigma} c^{\{0\}}_{vj\sigma} x_{pj\sigma}$$

Introducing the density matrices

$$\delta P^x_{qp\sigma} = \sum_{i\sigma} (x_{pi\sigma})^* x_{qi\sigma} + \sum_{rij} x_{rj\sigma} c^{\{0\}}_{pj\sigma} (c^{\{0\}}_{pj\sigma})^* (x_{ri\sigma})^*$$

$$\delta P^Z_{qp\sigma} = \sum_{i} Z_{pi\sigma} c^{\{0\}}_{qi\sigma}$$

Finally,

$$\omega^{(\eta)} = \sum_{pq\sigma} H^{(\eta)}_{pq\sigma} \left(\delta P^x_{qp\sigma} + \delta P^Z_{qp\sigma} \right)$$

For the full derivation see:

- F. Furche, R. Ahlrichs, J, Chem. Phys.,117 (2002) (localized basis sets)
- J. Hutter, J. Chem. Phys, 118, 3928 (2003) (plane wave basis sets)
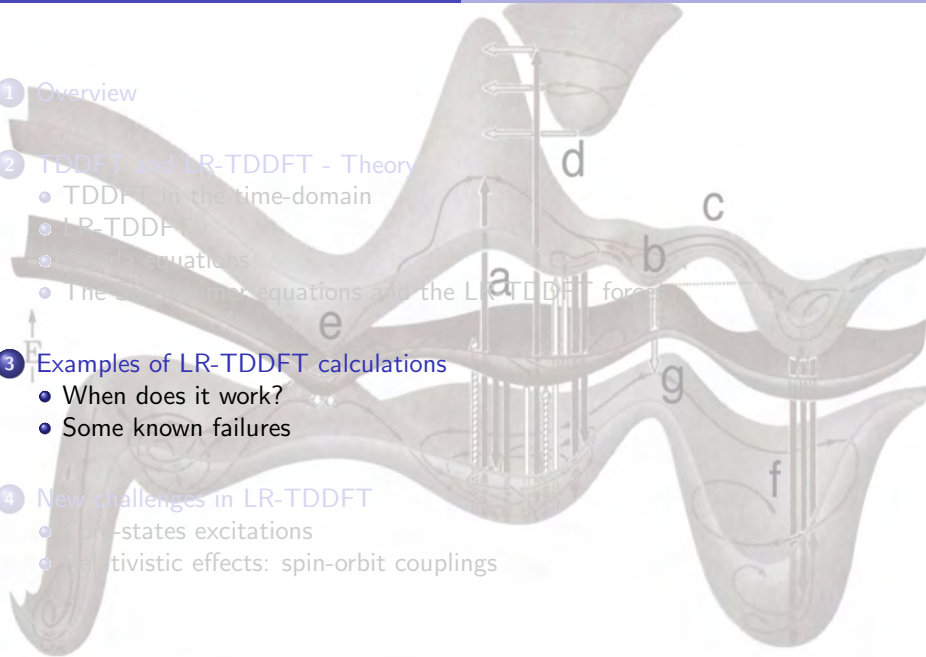
Benchmarks and references

"Extensive TD-DFT Benchmark: Singlet-Excited States of Organic Molecules"

Table 1. Training Set and Method Used in Recent Benchmark TD-DFT Calculations[a]

citation		training set			method				comparison
group(s)	ref.	states	molecules	functionals	basis set	solvent	transitions	geometry	
Boeij	14	25 mixed	19 molecules	SVWN, SVWN-VK	ET-pVQZ	none	vertical	BP/TZ2P	mixed[a]
Fabian	3	163 mixed	76 sulfur-bearing dyes	B3LYP	6-31+G(d)	none	vertical	B3LYP/6-31+G(d)	experiment
Fabian	12	54 mixed	21 sulfur-free dyes	B3LYP, B3LYP(TB)	6-31+G(d)	none	vertical	B3LYP/6-31+G(d)	experiment
Grimme	13	22 mixed	14 molecules	B3LYP	TZVP	none	vertical	B3LYP/TZVP	mixed
Grimme	63	42 $\pi - \pi^{*\,b}$	40 large molecules[c]	BP86, B3LYP, BHHLYP	TZVP	none[d]	0−0	DFT/TZVP	experiment[d]
Grimme	64	142/5 mixed	28/5 small/large molecules	6/17 functionals[e]	TZVP	none/PCM	vertical/0−0	MP2/DFT	theory[f]/experiment
Herbert	57	29 mixed	9 molecules	LC-PBE, LC-BLYP, LC-PBE0	aug-cc-PVDZ	none	vertical	B3LYP/6-31G(d)	experiment
Matsumura	7	50 $\pi - \pi^*$	50 organic dyes	B3LYP	6-31G(d), cc-pVDZ	none	vertical	B3LYP	experiment
Tozer	55	59 mixed	18 model molecules	PBE, B3LYP, CAM-B3LYP	cc-pVTZ[g]	none	vertical	Mixed[h]	mixed[i]
Thiel	62	102 mixed	28 small molecules	BP86, B3LYP, BHHLYP, MR-DFT	TZVP	none	vertical	MP2/6-31G(d)	theory[j]
Us	60	34 $n - \pi^*$	34 small dyes	12 pure and hybrid functionals[k]	Large w. diffuse[l]	PCM	vertical	PCM-DFT	experiment
Us	59	118 $\pi - \pi^*$	115 organic dyes	6 pure and hybrid functionals[m]	6-311++G(2d,p)	PCM	vertical	PCM-PBE0/6-311G(d,p)	experiment

[a] CAS-PT2, gas-phase measurements, or solvent measurements empirically corrected for solvatochromism. [b] Mainly $\pi - \pi^*$ transitions corresponding to singlet and doublet excited-states but a few other states. [c] Mainly aromatic and aliphatic hydrocarbons or oligomeric structures with a few heteroatoms. [d] No solvent model in the theory, but the experimental values have been shifted by a constant 0.15 eV (for all solvents) to include solvatochromism. [e] BP86, B3LYP, B2LYP, B2GPLYP, B2PLYP, and B2GP9LYP for the small molecules with PBE, OPBE, BLYP, mPWLYP, TPSS, VSXC, C3LYP, Bθ8, PBE0, BMK, and BHHLYP for the large ones. [f] CAS-PT2 from ref 9, using the same basis set and geometry. [g] d-aug-cc-pVTZ for Rydberg states. [h] Experimental, B3LYP/TZVP, CAM-B3LYP/6-31G(d), or MP2/6-31G(d) geometries, depending on the molecule. [i] Best estimates (generally CC3 or CAS-PT2) from their own ref 8, using the same basis set and geometry. [j] HF, BLYP, PBE, TPSS, B3LYP, PBE0, BMK, LC-BLYP, LC-PBE, LC-TPSS, LC-ωPBE, and CAM-B3LYP. [k] 6-311++G(3d,3p) for nitroso dyes and 6-311+G(2df,p) for thiocarbonyl chromophores. [l] HF, PBE, PBE0, LC-PBE, LC-ωPBE, and CAM-B3LYP. [m] For each contribution, we list the nature of the selected excited-state, molecules, and functionals as well as a summary of the methodological scheme. In this table, i) "basis set" refers to the basis set used for TD-DFT calculations; ii) "solvent" indicates the consideration or/not of environmental effects; iii) "transitions" indicates if full vibronic calculations have been computed or if vertical values have been used; iv) "geometry" gives the method used to obtain the molecular ground-state structures; and v) "comparison" indicates the origin of the values used as reference data during the statistical analysis.

JCTC, 5, 2420 (2009)

Organic dyes - Solvent effect

Organic Dyes for High-Performance Sensitized Solar Cells: the role of the solvent.

Table 1. Transition Energies (in eV) of the Dn Dyes in the Gas Phase and Ethanol Solution (SM8 solvation model) for All Studied Excited State Methods, Computed for the B3LYP/6-31G(d) SM8 Optimized Geometries with the 6-31+G(d) Basis Set

method	D5	D7	D9	D11
	Vacuum			
B3LYP	2.28	2.06	2.18	1.96
ωB97	3.10	3.09	3.03	2.96
ωB97X	3.04	3.01	2.96	2.88
CIS	3.24	3.23	3.19	3.13
SOS-CIS(D)	2.75	2.72	2.64	2.53
CIS(D)	2.92	2.89	2.82	2.72
	Ethanol, SM8			
B3LYP	2.16	2.07	1.98	1.88
ωB97	3.04	3.01	2.95	2.88
ωB97X	2.97	2.94	2.87	2.81
CIS	3.20	3.18	3.13	3.07
SOS-CIS(D)	2.59	2.56	2.43	2.35
SOS-CIS(D)[a]	2.72	2.68	2.59	2.48
CIS(D)	2.77	2.75	2.62	2.54
CIS(D)[a]	2.89	2.84	2.77	2.66
experimental	2.81	2.81	2.68	2.71

[a] The solvent effects in CIS second-order corrected methods were obtained from the gas phase vs SM8 differences obtained in CIS.
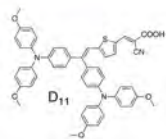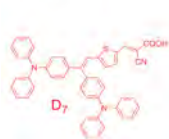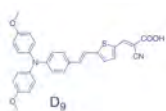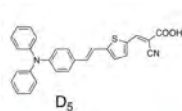
JCTC, 6, 1219 (2010)

Organometallic complex $(Mn_2(CO)_{10})$ - Structural effects
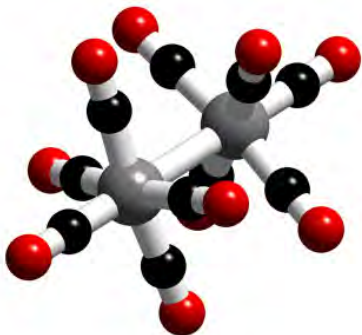
Structure and Bonding, 112, 49 (2004)

Organometallic complex $(Mn_2(CO)_{10})$ - Structural effects

Table 6 TDDFT/BP excitation energies (eV) and oscillator strengths (in parentheses) of the lowest allowed excited states of $Mn_2(CO)_{10}$, compared to experimental data and to ΔSCF-DFT and CASPT2 results

State	ΔSCF-DFT [68][a], [73][b]		TDDFT/BP [68][a]		CASPT2 [71][c]		Expt[d]
1^1E_1	3.07^a; 3.62^b	$d_\pi \rightarrow \sigma^*$	$3.22(0.007)^a$; $3.44(0.006)^c$; $3.35(0.006)^e$	$d_\pi \rightarrow \sigma^*$	$3.29(0.03)$	$d_\pi \rightarrow \sigma^*$	3.31
1^1B_2	2.95^a; 3.42^b	$\sigma \rightarrow \sigma^*$	$3.76(0.384)^a$; $4.01(0.252)^c$; $3.84(0.350)^e$	$\sigma \rightarrow \sigma^*$	$3.43(0.92)$	$\sigma \rightarrow \sigma^*$	3.69

[a] Becke-Perdew optimized geometry (see [81], Table 6, row 9); [b] Becke-Perdew optimized geometry; [c] X-ray structure from [82]; [d] solution spectrum of $Mn_2(CO)_{10}$ from [63]; [e] electron diffraction structure from [83]

- Very good agreement between TDDFT and CASPT2.
- However, result very sensitive to the molecular geometry.

Structure and Bonding, 112, 49 (2004)

A brief detour into ground state DFT

In 2006 J. Perdew has ordered the different *xc*-functional families on a Jacob's ladder. Each functional class represents a step towards the "heaven" of chemical accuracy.

LDA $\Rightarrow$ GGA $\Rightarrow$ meta-GGA $\Rightarrow$ Hybrids $\Rightarrow$ Others... (Double hybrids,...)

JCTC, 5, 902 (2009)

	Quantum chemical Heaven
double-hybrid	$\rho(\mathbf{r}), x(\mathbf{r}), \tau(\mathbf{r}), \psi_i(\mathbf{r}), \psi_a(\mathbf{r})$
RS-hybrids	$\rho(\mathbf{r}), x(\mathbf{r}), \tau(\mathbf{r}), \psi_i(\mathbf{r}), R_\alpha$
hybrids	$\rho(\mathbf{r}), x(\mathbf{r}), \tau(\mathbf{r}), \psi_i(\mathbf{r})$
mGGA	$\rho(\mathbf{r}), x(\mathbf{r}), \tau(\mathbf{r})$
GGA	$\rho(\mathbf{r}), x(\mathbf{r})$
LDA	$\rho(\mathbf{r})$

	Hartree world

Reduced gradient: $x(\mathbf{r}) = |\nabla \rho(\mathbf{r})|/\rho^{4/3}(\mathbf{r})$.
Local kinetic energy: $\tau(\mathbf{r}) = \sum_i n_i \psi_i(\mathbf{r}) \nabla^2 \psi_i((\mathbf{r}))$
Occupied, $\psi_i(\mathbf{r})$, and unoccupied, $\psi_a(\mathbf{r})$, KS orbitals.

RS: range-separated.

A brief detour into ground state DFT

Using a very large test set, Grimme *et al.* checked (computationally) the existence of the Jacob's ladder of functionals.
PCCP, 13, 6670 (2011)
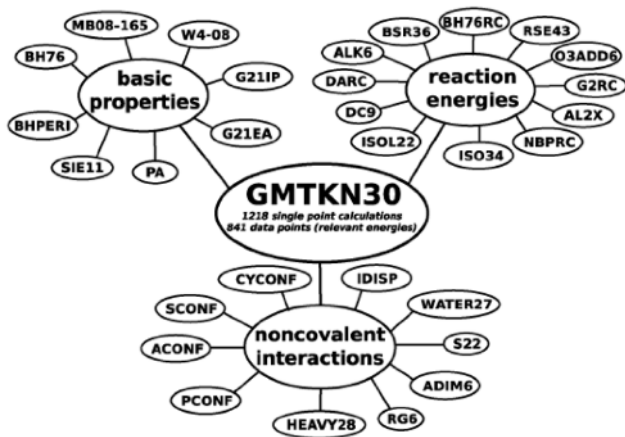
A brief detour into ground state DFT

Using a very large test set, Grimme *et al.* checked (computationally) the existence of the Jacob's ladder of functionals.
PCCP, 13, 6670 (2011)

1218 single point calculations and 841 data points (relative energies):

- Properties: atomization energies, electron affinities, ionization potentials, proton affinities, SIE related problems, barrier heights
- Various reaction energies: isomerizations, DielsAlder reactions, ozonolyses, reactions involving alkaline metals
- Noncovalent interactions: water clusters, conformational energies, and inter- and intra- molecular London-dispersion interactions

computed for **47** different *xc*-functionals

- 2 LDA
- 14 GGA
- 3 meta-GGA
- 23 hybrid
- 5 double-hybrid (DHDF) density functionals

A brief detour into ground state DFT

Using a very large test set, Grimme *et al.* checked (computationally) the existence of the Jacob's ladder of functionals.
PCCP, 13, 6670 (2011)

CAUTION:
Only closed-shell organic molecules have been considered!

A brief detour into ground state DFT

Using a very large test set, Grimme *et al.* checked (computationally) the existence of the Jacob's ladder of functionals.
PCCP, 13, 6670 (2011)

Jacob's ladder
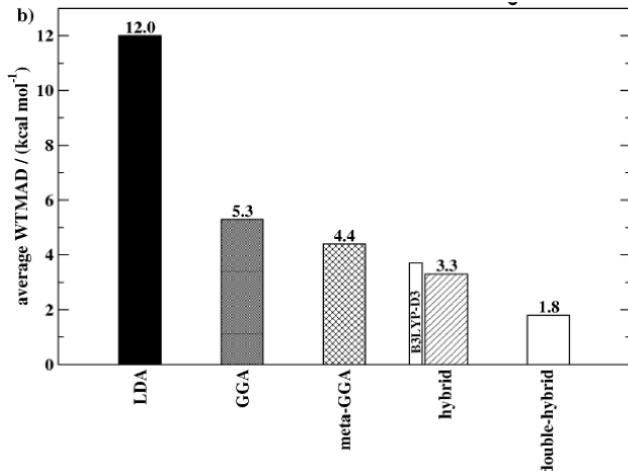
A brief detour into ground state DFT

Using a very large test set, Grimme *et al.* checked (computationally) the existence of the Jacob's ladder of functionals.
PCCP, 13, 6670 (2011)

GGA clearly improves over LDA - Only moderate improvement for meta-GGA
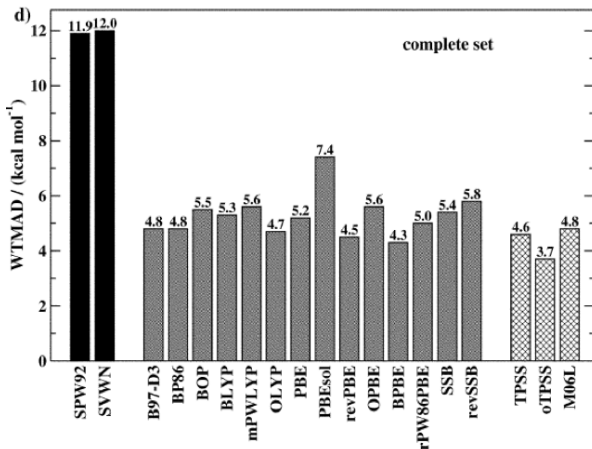
A brief detour into ground state DFT

Using a very large test set, Grimme *et al.* checked (computationally) the existence of the Jacob's ladder of functionals.
PCCP, 13, 6670 (2011)

Hybrid improves, but not as much as expected!
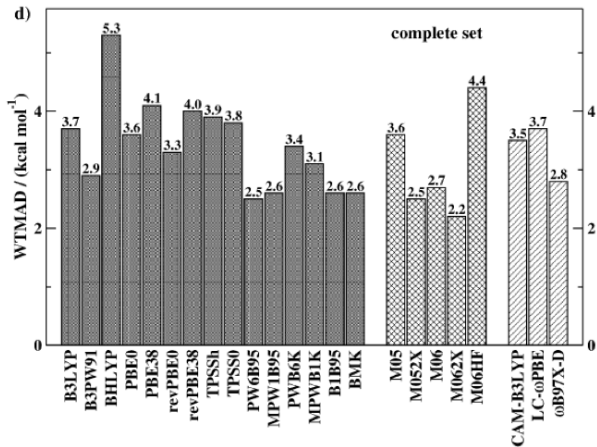
A brief detour into ground state DFT

Using a very large test set, Grimme *et al.* checked (computationally) the existence of the Jacob's ladder of functionals.
PCCP, 13, 6670 (2011)

Ground state DFT

Hybrid functionals improve only moderately compared to GGA functionals.

Back to LR-TDDFT

In TDDFT hybrid functionals may improve strongly compared to GGA

PCCP, 13, 16987 (2011)
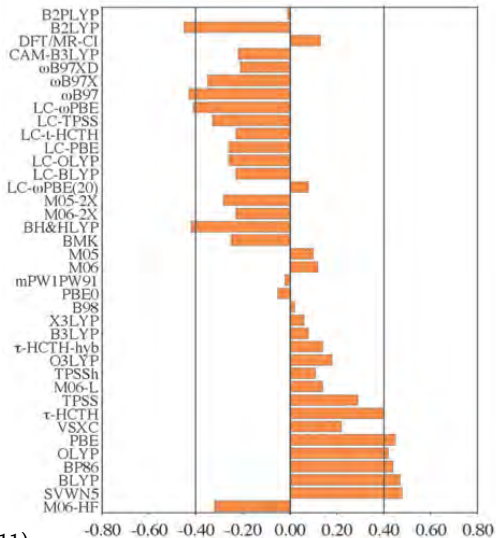
Choice of the *xc*-functional
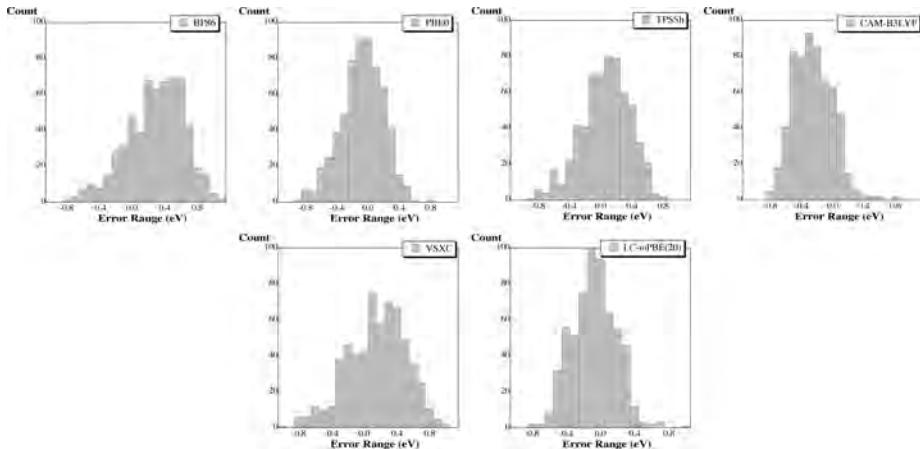
Figure: Histograms of the error for 614 excited states (VE = versus experiment)

JCTC, 5, 2420 (2009)

Choice of the *xc*-functional
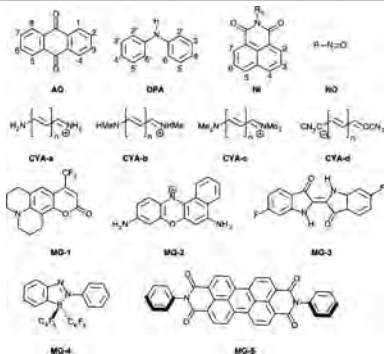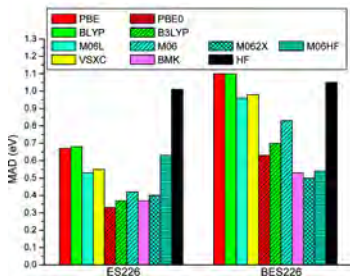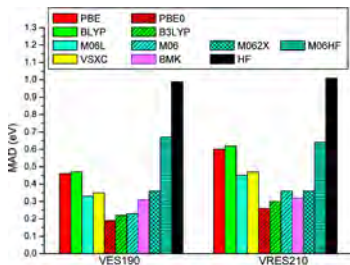
Figure: Examples of molecules in the VE test set.

Like for DFT: the quality of a functional depends on the *observable*
JCTC, 6, 2071 (2010)
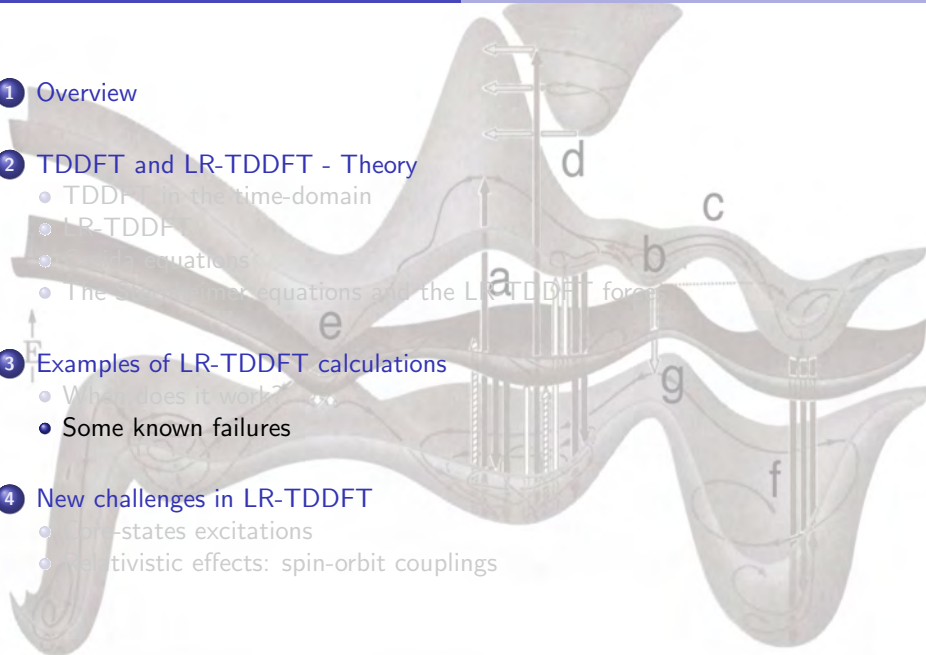
An important failure: charge transfer (CT) problem

Current *xc*-functionals usually underestimate dramatically charge transfer excitation state energies.

Charge transfer according to IUPAC

An electronic transition in which a large fraction of an electronic charge is transferred from one region of a molecular entity, called the electron donor, to another, called the electron acceptor (intramolecular CT) or from one molecular entity to another (intermolecular CT).

An important failure: charge transfer (CT) problem

Current *xc*-functionals usually underestimate dramatically charge transfer excitation state energies.
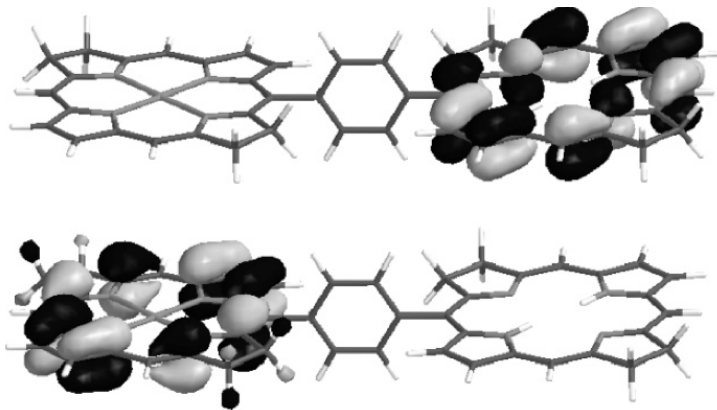
Figure: JACS,126, 4007 (2004)

An important failure: charge transfer (CT) problem

Current *xc*-functionals usually underestimate dramatically charge transfer excitation state energies.

TDDFT/BLYP   TDDFT with HF x
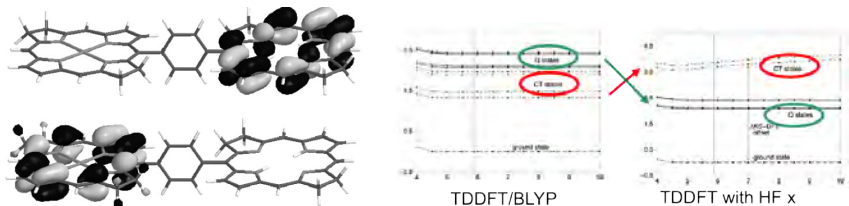
Figure: JACS,126, 4007 (2004)

How can we understand this failure?

$$A_{ia\sigma,jb\tau} = \delta_{\sigma\tau}\delta_{ij}\delta_{ab}(\epsilon_{a\sigma} - \epsilon_{i\sigma}) + (ia|f_H + f_{xc}^{\sigma\tau}|jb)$$

$$B_{ia\sigma,jb\tau} = (ia|f_H + f_{xc}^{\sigma\tau}|bj)$$

An important failure: charge transfer (CT) problem

Current *xc*-functionals usually underestimate dramatically charge transfer excitation state energies.

TDDFT/BLYP   TDDFT with HF x
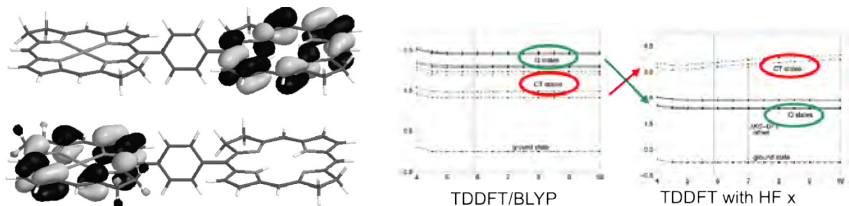
Figure: JACS,126, 4007 (2004)

How can we understand this failure? For ψ_i and ψ_a with no overlap :

$$A_{ia\sigma,jb\tau} = \delta_{\sigma\tau}\delta_{ij}\delta_{ab}(\epsilon_{a\sigma} - \epsilon_{i\sigma}) + \underbrace{(ia|f_H + f_{xc}^{\sigma\tau}|jb)}$$

$$B_{ia\sigma,jb\tau} = \underbrace{(ia|f_H + f_{xc}^{\sigma\tau}|bj)}$$

An important failure: charge transfer (CT) problem

Current *xc*-functionals usually underestimate dramatically charge transfer excitation state energies.

TDDFT/BLYP   TDDFT with HF x
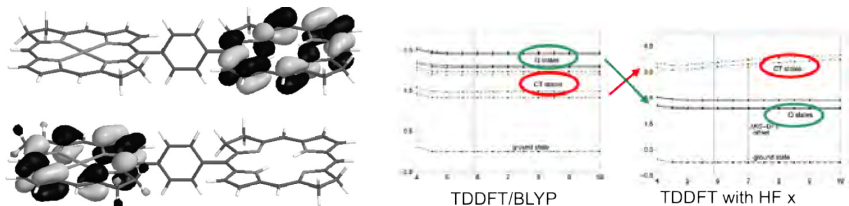
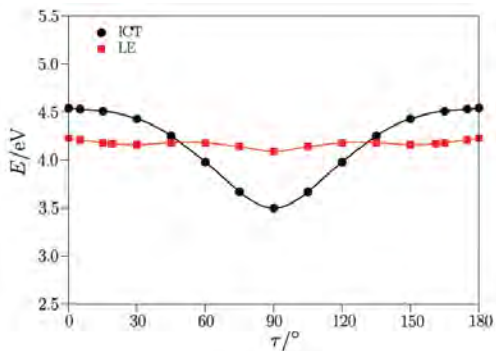Figure: JACS,126, 4007 (2004)

We are left with orbital energy differences.

Example of CT problem

N,N-dimethylaminobenzonitrile (DMABN) - Complete analysis by Tozer *et al.* JCP, 131, 091101 (2009)

CC2 (wavefunction-based method)
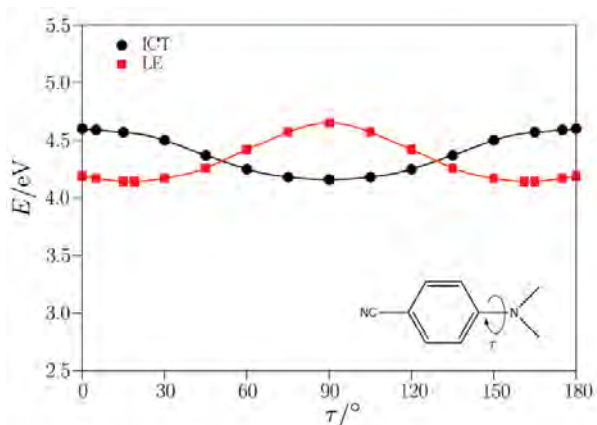
Example of CT problem

N,N-dimethylaminobenzonitrile (DMABN) - Complete analysis by Tozer *et al.* JCP, 131, 091101 (2009)


$\tau = 0^{\circ}$

Example of CT problem

N,N-dimethylaminobenzonitrile (DMABN) - Complete analysis by Tozer *et al.* JCP, 131, 091101 (2009)

$\tau = 90°$
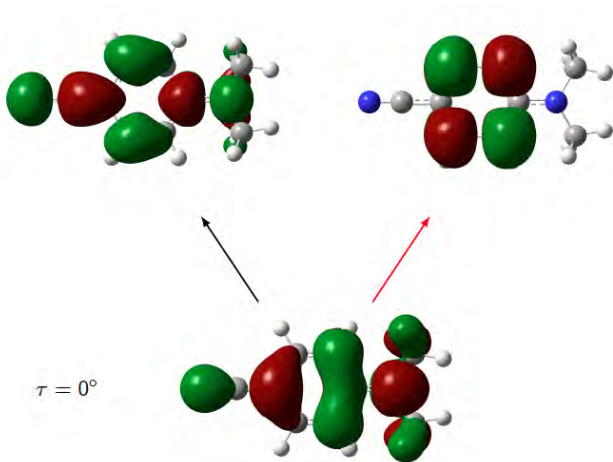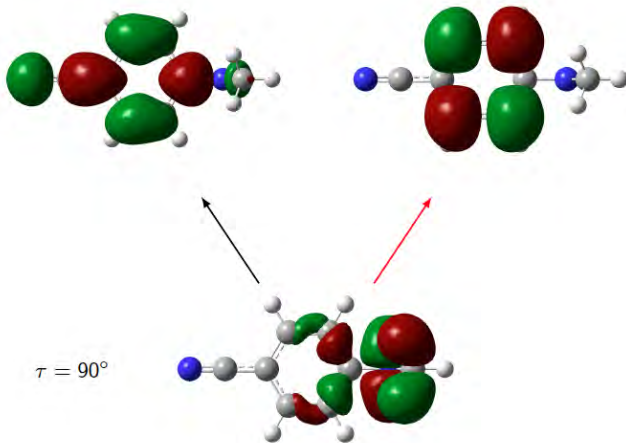
Example of CT problem

N,N-dimethylaminobenzonitrile (DMABN) - Complete analysis by Tozer *et al.* JCP, 131, 091101 (2009)

PBE
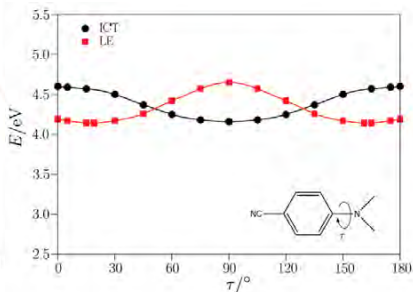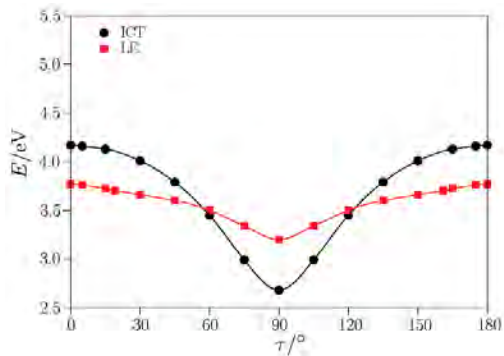
Example of CT problem

N,N-dimethylaminobenzonitrile (DMABN) - Complete analysis by Tozer *et al.* JCP, 131, 091101 (2009)

B3LYP
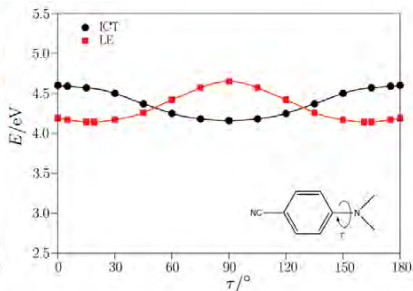
Example of CT problem

N,N-dimethylaminobenzonitrile (DMABN) - Complete analysis by Tozer *et al.* JCP, 131, 091101 (2009)

CAM-B3LYP
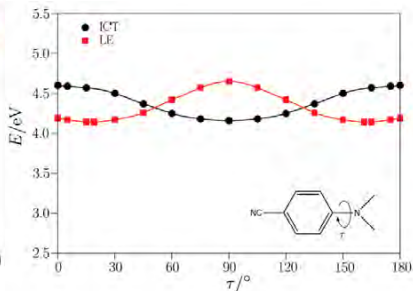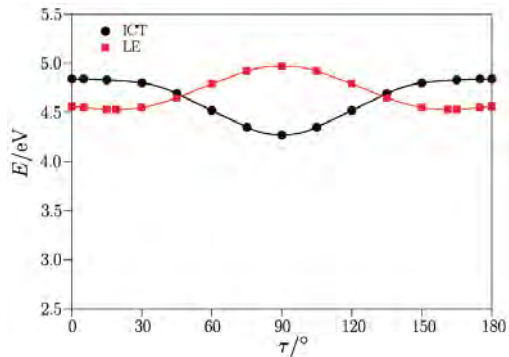
Failures of *xc*-functionals for charge transfer states.

(a) RI-CC2

(b) PBE

(c) B3LYP

(d) CAM-B3LYP
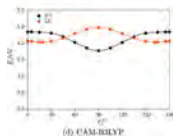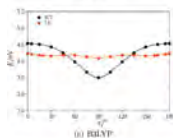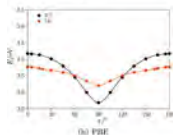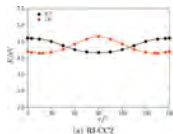
- CT failures may affect dramatically the shape of the PESs.
- CT failures may affect the ordering of the electronic states.
- The quality of PESs is not uniformly spread over the entire configuration space.
- Dramatic for dynamics on excited states.
- Hopes from better new *xc*-functionals.

CAUTION

# Adiabatic approximation: the problem of double excitations

Due to the adiabatic approximation (frequency independent kernel: Casida equation gives solutions with single-electron excitation character), double excitation characters are not properly captured.

$$f_{xc}^{\sigma\tau}(\mathbf{r}t, \mathbf{r}'t') = \delta(t - t') \frac{\delta^2 E_{xc}[\rho]}{\delta\rho_\sigma(\mathbf{r})\delta\rho_\tau(\mathbf{r}')}.$$

Typical examples: butadiene excitation energies of single excitation character are well reproduced (1^1B_u), not those with double excitation character (2^1A_g and 4^1A_g).

- black square: TDDFT/B3LYP
- gray line: CAS(4/4)*PT2

In fact, the 2^1A_g state from TDDFT is more similar in behaviour to the 3^1A_g state from CASPT2. This suggests that TDDFT with the current array of approximate functionals is incapable of reproducing the state with significant doubly excited character.

Mol. Phys., 104, 1039 (2006)

Bond alternation / angstorm
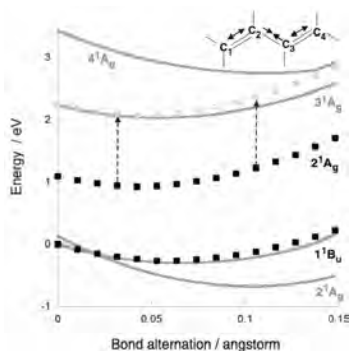
Topology of the excited states

Photochemistry/photophysics require a correct description of the topological properties of the most relevant potential energy surfaces involved.

Conical intersections are now recognized to play a critical role in the reaction dynamics of electronic excited states.

They occur at geometries for which two electronic states are exactly degenerate.
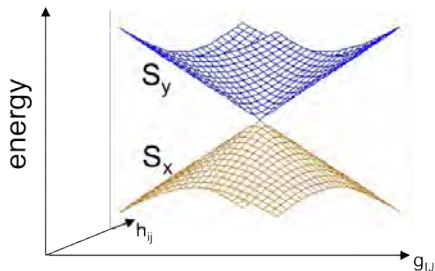
Branching space is composed by the **gradient difference $\mathbf{g}_{IJ}$** and the **nonadiabatic coupling vector $\mathbf{h}_{IJ}$**.

$$\mathbf{g}_{IJ} = \nabla_{\mathbf{R}}(E_I - E_J)$$
$$\mathbf{h}_{IJ} = \langle \Phi_I | \nabla_{\mathbf{R}} | \Phi_J \rangle$$

Topology of the excited states

What about the topology of the TDDFT PESs close to a conical intersection?

Formally, TDDFT equations in the Tamm-Dancoff approximation (TDA) are similar to the CIS equations for the excited state energies.
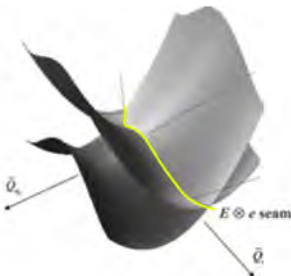
By applying Brillouin's theorem, one can show that restricted CIS (for closed shell systems) has the wrong dimensionality for the intersection with the S_0 PES: $f - 1$ (a seam of intersections instead of a conical intersection).

Topology of the excited states

What about the topology of the TDDFT PESs close to a conical intersection?

Formally, TDDFT equations in the Tamm-Dancoff approximation (TDA) are similar to the CIS equations for the excited state energies.

By applying Brillouin's theorem, one can show that restricted CIS (for closed shell systems) has the wrong dimensionality for the intersection with the S_0 PES: $f - 1$ (a seam of intersections instead of a conical intersection).

Topology of the excited states

What about the topology of the TDDFT PESs close to a conical intersection?

Formally, TDDFT equations in the Tamm-Dancoff approximation (TDA) are similar to the CIS equations for the excited state energies.

By applying Brillouin's theorem, one can show that restricted CIS (for closed shell systems) has the wrong dimensionality for the intersection with the S_0 PES: $f - 1$ (a seam of intersections instead of a conical intersection).

Why is it the case?

For a simple two level system, the adiabatic energies of each state are described by:

$$E_{0,1} = (H_{00} + H_{11})/2 \pm \sqrt{((H_{00} - H_{11})/2)^2 + H_{01}^2}.$$

Topology of the excited states

What about the topology of the TDDFT PESs close to a conical intersection?

Formally, TDDFT equations in the Tamm-Dancoff approximation (TDA) are similar to the CIS equations for the excited state energies.
By applying Brillouin's theorem, one can show that restricted CIS (for closed shell systems) has the wrong dimensionality for the intersection with the S_0 PES: $f - 1$ (a seam of intersections instead of a conical intersection).

Why is it the case?

For a simple two level system, the adiabatic energies of each state are described by:

$$E_{0,1} = \left(H_{00} + H_{11} \right)/2 \pm \sqrt{\left(\left(H_{00} - H_{11} \right)/2 \right)^2 + H_{01}^2}\,.$$

The conditions for a conical intersection are: $(H_{00}(\mathbf{R}) - H_{11}(\mathbf{R})) = 0$ and $H_{01}(\mathbf{R}) = 0$, i.e. imply generally two constraints. However, from Brillouin's theorem, we know that the matrix elements $H_{01} = \langle \Phi_0 | \hat{\mathcal{H}}_{el} | \Phi_1 \rangle$ are always zero, therefore there is only one condition to satisfy and the CI is described in a f-1 space.
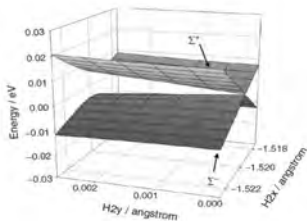
Topology of the excited states

What about the topology of the TDDFT PESs close to a conical intersection?

Formally, TDDFT equations in the Tamm-Dancoff approximation (TDA) are similar to the CIS equations for the excited state energies.

By applying Brillouin's theorem, one can show that restricted CIS (for closed shell systems) has the wrong dimensionality for the intersection with the S_0 PES: $f - 1$ (a seam of intersections instead of a conical intersection).

Why is it the case?

For a simple two level system, the adiabatic energies of each state are described by:

$$E_{0,1} = \left(H_{00} + H_{11}\right)/2 \pm \sqrt{\left(\left(H_{00} - H_{11}\right)/2\right)^2 + H_{01}^2} \,.$$

The conditions for a conical intersection are: $(H_{00}(\mathbf{R}) - H_{11}(\mathbf{R})) = 0$ and $H_{01}(\mathbf{R}) = 0$, i.e. imply generally two constraints. However, from Brillouin's theorem, we know that the matrix elements $H_{01} = \langle \Phi_0 | \hat{\mathcal{H}}_{el} | \Phi_1 \rangle$ are always zero, therefore there is only one condition to satisfy and the CI is described in a f-1 space.
Is this also the case in TDDFT?

Topology of the excited states

S_0/S_1 **intersection in linear water** (Mol. Phys., 104, 1039 (2006))
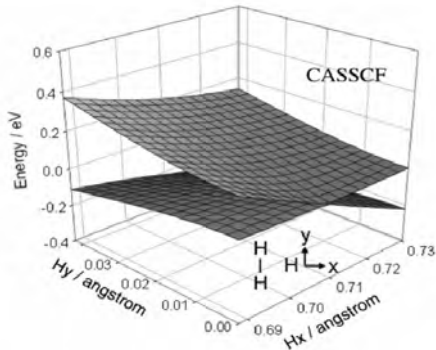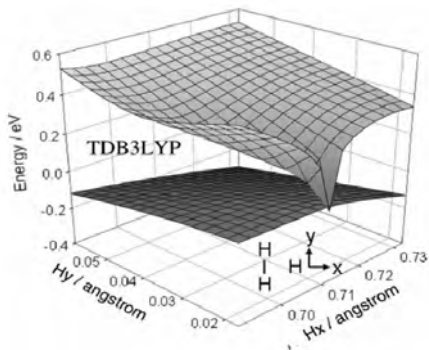CIS - TDDFT
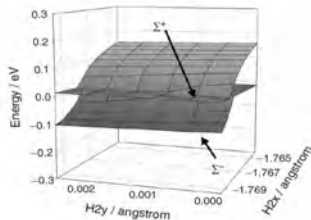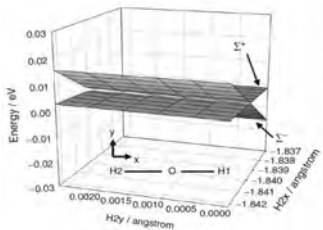
CASSCF

Topology of the excited states
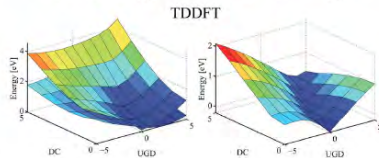
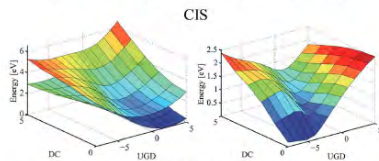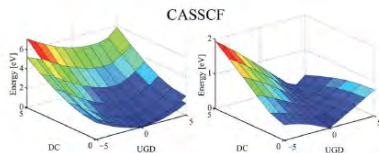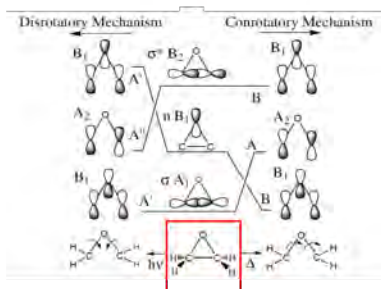S_0/S_1 **for** $H_2 + H$ (Mol. Phys., 104, 1039 (2006))

TDDFT - CASSCF

TDDFT seems to reproduce the correct splitting of the surfaces.
However, slope around the CI is much steeper...

Topology of the excited states

... but it is not a general failure of TDDFT

Ref: *J. Chem. Phys.* **129**, 124108 (2008).

Short summary - LR-TDDFT for excitation energies

- For valence excited states well below the ionization potential ($\sim -\epsilon_{HOMO}$) $\Rightarrow$ error between 0.2 and 0.6 eV (0.1 eV $\approx$ 10 kJ/mol).
- Good ordering and relative energies of the excited states (except for CT states).
- Good also for transition metals (difficult for wavefunction based methods).
- Scales $\sim$ like $O(n^2)$ with n the number of electrons: can deal with very large systems up to many hundreds of atoms.

- Many times, TDDFT properties are bad because the underlying DFT is inaccurate (bond dissociations, biradicals, self-interaction error, ...).
- Topology of the excited surfaces is not always correct.
- Problems to describe double excitations, Rydberg excited states, large π systems.
- Standard xc functionals fail in the case of CT states.
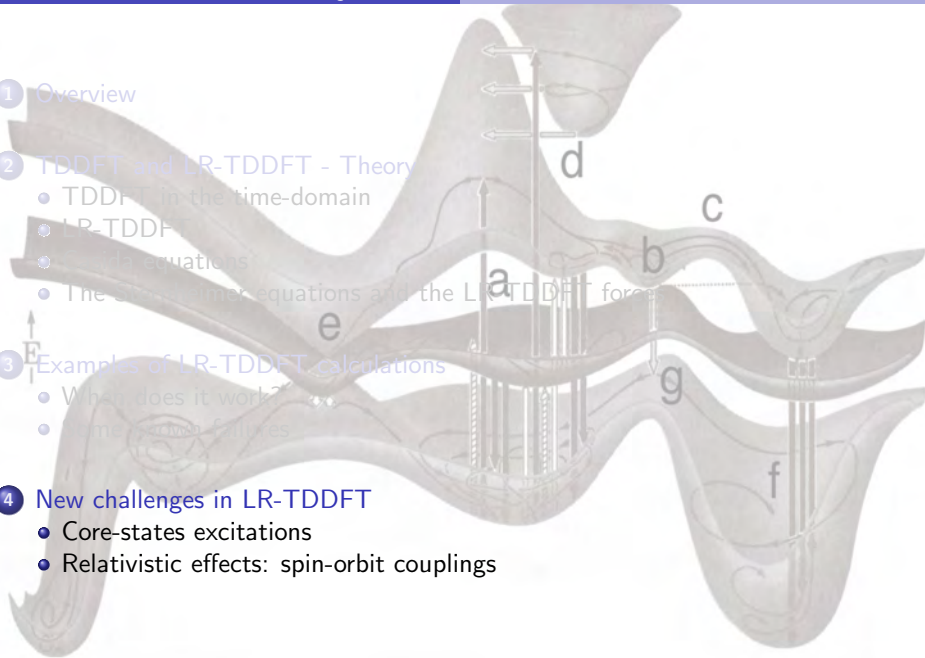- Errors in the ordering of the excited PESs is deleterious for excited states MD.

Core excitations: XANES and EXAFS spectra
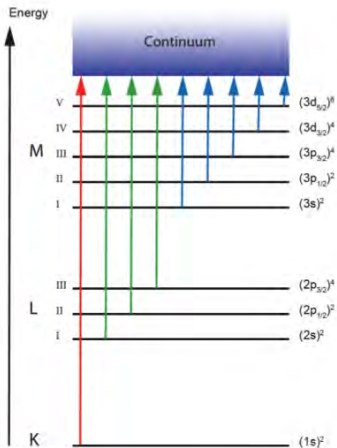
Core excitations are dealing with excitations from core states (K, L, M shells) into resonant states and continuum.

Experimentally, two techniques were developed:

XANES: X-ray absorption near-edge structure.
It typically lies within the first 30 eV of the edge position. Dominated by Multi Scattering (MS) events.

EXAFS: extended X-ray absorption fine structure.
Excess photoelectron energy is large and single-scattering (SS) events dominate. This makes the interpretation simpler.

Core excitations: XANES and EXAFS spectra

Interpretation: MS and SS events provide information of the molecular structure.
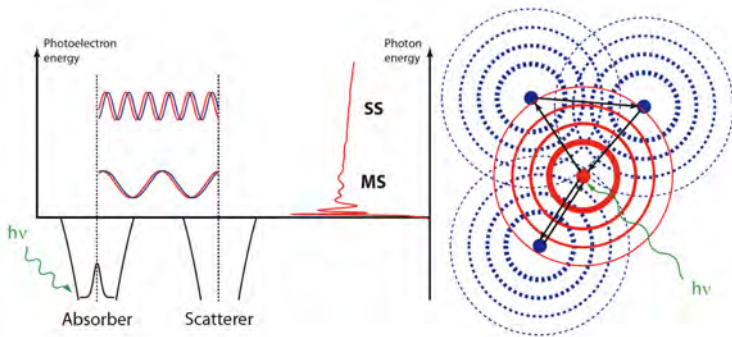
XAFS originates from interference effects in the scattering of the photoelectron from neighboring atoms. Multi Scattering / Single Scattering events dominate at low / high photoelectron energies. SS and MS events (black arrows) leading to interference of the outgoing (red) and the scattered (blue) photoelectron waves at the absorber.

Experimental studies: XANES and EXAFS spectra
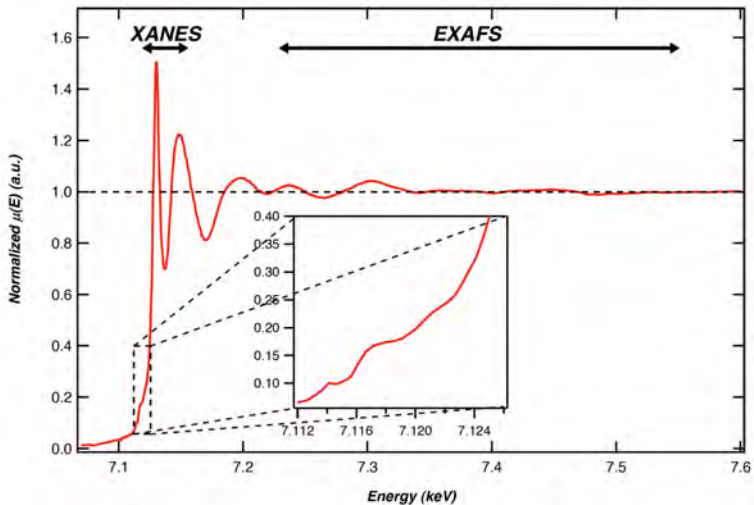
Core excitations: a challenge for TDDFT

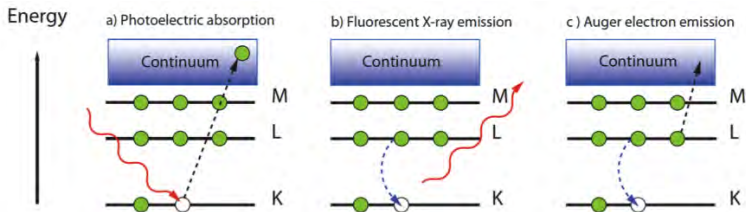Core excitations give rise to very complex electronic reorganization processes, which are a challenge for TDDFT.

Relaxation processes following the creation of a core-hole (a):
(b) The core-hole can be filled via radiative processes
(c) The core-hole can be filled via Auger electron production.

XANES/EXAFS energies for metal complexes are in the order of several keV and the typical TDDFT errors are of about 100 eV.

Fortunately the error is mainly a constant shift.

Core excitations: a challenge for TDDFT

[Gloria Capano, Thomas Penfold; Majed Chergui]
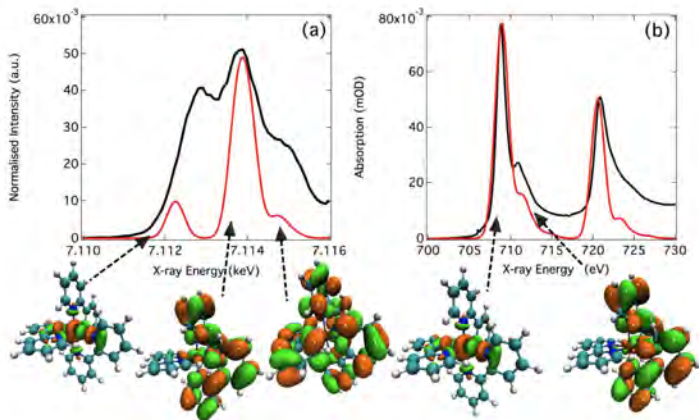
(a) The pre-edge region of the Fe K-edge of $[Fe(bpy)_3]^{2+}$ and (b) the $L_{2/3}$-edge spectrum for low spin. The important molecular orbital are shown beneath. [*Chem. Phys. Chem.*, **580**, 179 (2013)]

From Dirac equation to relativistic DFT/TDDFT

The starting point is the 4-component relativistic Dirac equation

$$\left(\beta mc^2 + c \sum_{k=1}^{3} \alpha_k p_k \right) \psi(x, t) = i\hbar \frac{\partial \psi(x, t)}{\partial t}$$
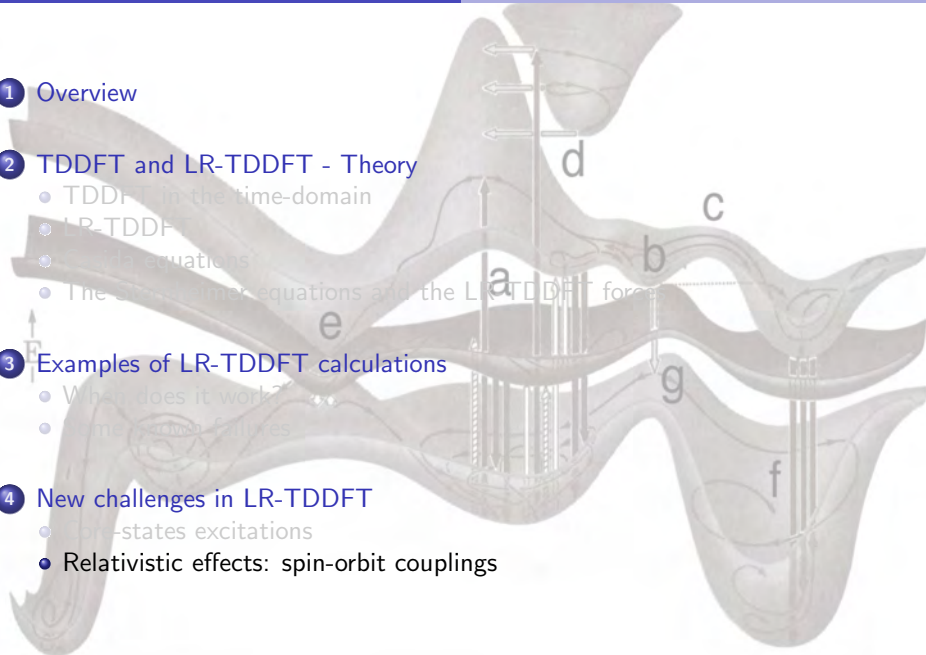
The *densityfunctionalization* of this equation can occur mainly following two paths:

- Densityfunctionalization of the 4− (or 2−) component Dirac equation. *Chapter 8 in R.M. Dreitzler and E.K.U. Grosss, Density Functional Theory, Springer Verlag.*

- Compute perturbatively the first order correction of the nonrelativistic Hamiltonian and then do its densityfunctionalization:

$$\langle \Psi_I(\mathbf{r}_1, \ldots, \mathbf{r}_N)| \frac{\alpha^2}{2} \left[\sum_{\gamma=1}^{N_\gamma} \sum_{i=1}^{N_{el}} Z_\gamma \left(\frac{\mathbf{r}_{i\gamma}}{r_{i\gamma}} \times \mathbf{p}_i \right) \cdot \mathbf{s}_i \right] |\Psi_J(\mathbf{r}_1, \ldots, \mathbf{r}_N)\rangle .$$

Auxiliary wavefunctions for LR-TDDFT

It is possible to express linear response quantities within TDDFT using a set of auxiliary many-electron wavefunctions.

They are given as a linear combination of singly excited Slater determinants

The auxiliary many-electron wavefunctions (AX WF)

$$\tilde{\Psi}_I[\{\phi.\}] = \sum_{ia\sigma} c^I_{ia\sigma} \, \hat{a}^\dagger_{a\sigma} \hat{a}_{i\sigma} \tilde{\Psi}_0[\{\phi.\}]$$

with

$$c^I_{ia\sigma} \equiv \sqrt{\frac{S^{-1}_{ia\sigma}}{\omega_{0I}}} e^I_{ia\sigma}$$

where $\tilde{\Psi}_0[\{\phi.\}]$ is the Slater determinant of all occupied KS orbitals $\{\phi_{i\sigma}\}^N_{i=1}$, and $\hat{a}^\dagger_{a\sigma}$, $\hat{a}_{i\sigma}$ are the creation (of virtual orbitals, $\phi_{a\sigma}$) and annihilation operators.

I.T., E. Tapavicza, U. Rothlisberger, JCP, **130**, 124107 (2007)
I.T., B. F. E. Curchod, U. Rothlisberger, JCP, **131**, 196101 (2009)

I.T., B. F. E. Curchod, A. Laktionov, U. Rothlisberger, JCP, **133**, 194104 (2010)

Collinear DFT/TDDFT and its limits

In the collinear LSDA approximation, each electronic spin is oriented along a fixed quantization axis (z-axis) and therefore the spinors can be written in the spin-up (α) and spin-down (β) forms

$$\psi_{i,\alpha}(\mathbf{r}) = \begin{pmatrix} \psi_i(\mathbf{r}, \alpha) \\ 0 \end{pmatrix}, \quad \psi_{j,\beta}(\mathbf{r}) = \begin{pmatrix} 0 \\ \psi_i(\mathbf{r}, \beta) \end{pmatrix}$$

or in the direct product space spanned by the Hilbert space of the KS-orbitals, H_{KS} and the two-dimensional spin space H_{Spin}, as

$$\psi_{i,\alpha}(\mathbf{r}) = \psi_i(\mathbf{r}) \otimes \begin{pmatrix} 1 \\ 0 \end{pmatrix}, \quad \psi_{j,\beta}(\mathbf{r}) = \psi_i(\mathbf{r}) \otimes \begin{pmatrix} 0 \\ 1 \end{pmatrix}$$

The spin magnetization then becomes simply

$$m_z(\mathbf{r}) = \mu_B \left[\sum_i^{N_\alpha} |\psi_{i,\alpha}(\mathbf{r})|^2 - \sum_i^{N_\beta} |\psi_{i,\beta}(\mathbf{r})|^2 \right]$$

and $m_x(\mathbf{r}) = m_y(\mathbf{r}) = 0$, where N_α and N_β are the number of occupied α and β KS orbitals, respectively.

Limits of collinear DFT/TDDFT: $M_S = 0$

The solution to the collinear case of the LR-TDDFT equations and the corresponding AMEWs can be associated to spin-adapted configurations (eigenvectors of the $\mathbf{S}^2$ operator) with $M_S = 0$:

$$\text{singlet: } \frac{1}{\sqrt{2}}(|\alpha\beta\rangle - |\beta\alpha\rangle) \quad \text{and} \quad \text{triplet: } \frac{1}{\sqrt{2}}(|\alpha\beta\rangle + |\beta\alpha\rangle).$$

The singlet and triplet excited state AMEW will be given by

$$|S_1^0\rangle = \sum_i^N \sum_{\xi=\alpha,\beta} (\hat{r}_{i\xi}^S)^\dagger \hat{a}_{i\xi}|\Psi_0\rangle \,,$$

and

$$|T_1^0\rangle = \sum_i^N (\hat{r}_{i\alpha}^T)^\dagger \hat{a}_{i\alpha}|\Psi_0\rangle - (\hat{r}_{i\beta}^T)^\dagger \hat{a}_{i\beta}|\Psi_0\rangle \,,$$

respectively.

The "spin-flip" transition: the noncollinear solutions

In conventional, collinear LR-TDDFT, only the $M_S = 0$ component of each triplet state can be obtained, as the attainment of $M_S = -1$ or $M_S = +1$ states necessitates spin-flip excitations to be taken into account

Wang and Ziegler, *J. Chem. Phys.*, **121**, 12191 (2004).

$$n(\mathbf{r}) = \sum_{i=1}^{N} \begin{pmatrix} |\phi_{i\uparrow}^0(\mathbf{r})|^2 & \phi_{i\uparrow}^0(\mathbf{r})\phi_{i\downarrow}^{0*}(\mathbf{r}) \\ \phi_{i\downarrow}^0(\mathbf{r})\phi_{i\uparrow}^{0*}(\mathbf{r}) & |\phi_{i\downarrow}^0(\mathbf{r})|^2 \end{pmatrix} , \qquad \boldsymbol{\xi}_0(\mathbf{r}) = \frac{Tr[\boldsymbol{\sigma}\mathbf{n}]}{n_0(\mathbf{r})} ,$$

we get

$$v_{xc,\sigma\sigma'}^0(\mathbf{r}) = \frac{\delta E_{xc}[n, \boldsymbol{\xi}]}{\delta n_{\sigma\sigma'}^0(\mathbf{r})}$$
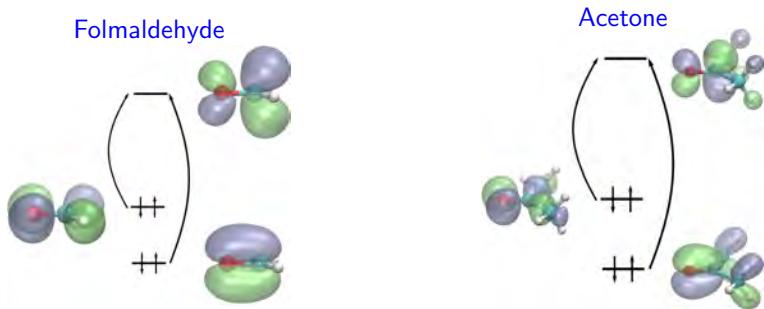
$$f_{\uparrow\uparrow,\uparrow\uparrow}^{xc} = \frac{\partial^2(n e_{xc}^h)}{\partial n^2} + 2(1-\xi)\frac{\partial^2 e_{xc}^h}{\partial n \partial \xi} + \frac{(1-\xi)^2}{n}\frac{\partial^2 e_{xc}^h}{\partial \xi^2}$$

$$\vdots$$

$$f_{\uparrow\downarrow,\uparrow\downarrow}^{xc} = \frac{2}{n\xi}\frac{\partial e_{xc}^h(n, \xi)}{\partial \xi}$$

Test applications: formaldehyde and acetone

- collinear LR-TDDFT
- molecules oriented such that only $M_S = 0$ component of the SOC is nonvanishing
- matrix elements computed using the auxiliary many-electron wavefucntion

Folmaldehyde

Acetone

Test applications: formaldehyde and acetone

Transitions	$\|\langle^1(n,\pi^*)\|\|^3(\pi,\pi^*)_0\rangle\|$	$\|\langle^1(n,\pi^*)\|\|^3(\pi,\pi^*)_{+1}\rangle\|$	$\|\langle^1(n,\pi^*)\|\|^3(\pi,\pi^*)_{-1}\rangle\|$	Total
formaldehyde (strong coupling)				
SO-GMCQDPT2	102.6149	0.0010	0.0010	102.6149
LR-TDDFT/PBE (l)	92.9600	0.0001	0.0141	92.9737
LR-TDDFT/PBE (h)	101.6651	0.0069	0.0069	101.6651
acetone (strong coupling)				
SO-GMCQDPT2	90.9543	0.0118	0.0118	90.9543
LR-TDDFT/PBE (l)	85.4613	0.0047	0.0048	85.4189
LR-TDDFT/PBE (h)	97.5095	0.0044	0.0044	97.5095
Transitions	$\|\langle^1(\pi,\pi^*)\|\|^3(\pi,\pi^*)_0\rangle\|$	$\|\langle^1(\pi,\pi^*)\|\|^3(\pi,\pi^*)_{+1}\rangle\|$	$\|\langle^1(\pi,\pi^*)\|\|^3(\pi,\pi^*)_{-1}\rangle\|$	Total
formaldehyde (weak coupling)				
SO-GMCQDPT2	0.0000	0.0016	0.0016	0.0023
LR-TDDFT/PBE (l)	0.0011	0.0006	0.0022	0.0031
acetone (weak coupling)				
SO-GMCQDPT2	0.0000	0.0023	0.0023	0.0032
LR-TDDFT/PBE (l)	0.0086	0.0001	0.0001	0.0086

Rigorous derivation of SOC in LR-TDDFT

More will come soon especially in relation to "spin-flip" transition.
.... we will have soon a publication on this subject ...